SYSTEM DESIGN AND OPTIMIZATION OF CO_2 STORAGE IN DEEP SALINE AQUIFERS

A Thesis

by

HOSSEIN SHAMSHIRI

Submitted to the Office of Graduate Studies of
Texas A&M University
in partial fulfillment of the requirements for the degree of

MASTER OF SCIENCE

December 2010

Major Subject: Petroleum Engineering

System design and Optimization of CO_2 Storage in Deep Saline Aquifers

SYSTEM DESIGN AND OPTIMIZATION OF CO_2 STORAGE IN DEEP SALINE AQUIFERS

A Thesis

by

HOSSEIN SHAMSHIRI

Submitted to the Office of Graduate Studies of
Texas A&M University
in partial fulfillment of the requirements for the degree of

MASTER OF SCIENCE

Approved by:

Chair of Committee,	Yousef Jafarpour
Committee Members,	Eduardo Gildin
	Shankar P. Bhattacharyya
Head of Department,	Steve Holditch

December 2010

Major Subject: Petroleum Engineering

ABSTRACT

System Design and Optimization of CO_2 Storage in

Deep Saline Aquifers. (December 2010)

Hossein Shamshiri, B.S., Petroleum University of Technology

Chair of Advisory Committee: Dr. Yousef Jafarpour

Optimization of waterflooding sweep efficiency has been widely applied in reservoir engineering to improve hydrocarbon recovery while delaying water breakthrough and minimizing the bypassed oil in reservoirs. We develop a new framework to optimize flooding sweep efficiency in geologic formations with heterogeneous properties and demonstrate its application to waterflooding and geological CO_2 sequestration problems. The new method focuses on equalizing and delaying (under constant total injected volume) the breakthrough time of the injected fluid at production wells. For application to CO_2 sequestration where producers may not be present, we introduce the concept of pseudo production wells that have insignificant production rates (with negligible effect on the overall flow regime) for quantification of hypothetical breakthrough curves that can be used for optimization purpose. We apply the new method to waterflooding and CO_2 sequestration optimization using two heterogeneous reservoir models. We show that in water flooding experiments, the proposed method improves the sweep efficiency by delaying the field breakthrough and equalizing breakthrough times in all production wells. In this case, the optimization results in increased oil recovery and decreased water production. We apply a modified version of the proposed algorithm to geologic CO_2 sequestration problems to maximize the storage capacity of aquifers by enhancing the residual and dissolution trapping. The results from applying the proposed approach to optimization of geologic CO_2 storage problems illustrate the effectiveness of the algorithm in improving residual and solubility trapping by increasing the contact

between available fresh brine and the injected CO_2 plume through a more uniform distribution of CO_2 in the aquifer.

DEDICATION

To my parents, family, teachers and friends

ACKNOWLEDGEMENTS

First, I would like to acknowledge my gratitude to Dr. B. Jafarpour for his supervision, advice, and guidance from the very early stage of this research as well as giving me extraordinary experiences throughout the work. Above all and the most needed, he provided me unflinching encouragement and support in various ways. His truly scientist intuition has made him as a constant oasis of ideas and passion in science, which exceptionally inspire and enrich my growth as a student and a researcher. I am indebted to him more than he knows.

Many thanks go in particular to Dr. E. Gildin and Dr. Shankar P. Bhattacharyya. I am indebted to them for their valuable advice in discussions, supervision and furthermore, using their precious time to read this thesis and giving their critical comments about it.

The waterflooding and geologic CO_2 storage simulations in this study were carried out using Schlumberger's Geoquest Eclipse© reservoir simulation package. Therefore, I would like to express my appreciation to the Schlumberger's software group for providing the uninterrupted license of the software packages.

Where would I be without my family? My parents deserve special mention for their inseparable support and prayers. My father is the person who put the fundamentals in my learning character, showing me the joy of intellectual pursuit ever since I was a child. My mother, is the one who lovingly raised me with her caring and gentle love.

Last but not least, I would like to thank all my friends who helped me and have been supportive to me during this study, especially my dear girlfriend, Laura Flores, who really made a nice environment for me to work on my thesis; she is nice, kind and lovely, and I will always have her in my heart.

TABLE OF CONTENTS

Page

Page

LIST OF FIGURES

Page

Page

Page

LIST OF TABLES

Page

CHAPTER I

INTRODUCTION AND LITERATURE REVIEW

1.1 CO_2 SEQUESTRATION

The pressing need for a clean and renewable energy infrastructure is primarily driven by the worldwide depletion of easily recoverable fossil fuel resources and the alarming trends in climate change and environmental degradation. According to the United Nations Intergovernmental Panel for Climate Change (IPCC, 2005), today, approximately 80% of the global energy consumption is supplied by fossil fuels, a fact that does not seem to change for the near future. The existing evidence suggests that the move toward clean and sustainable energy resources is likely to be fueled mainly by carbon-based fossil energy sources, which has called for controlled emission of anthropogenic carbon dioxide (CO_2) into the atmosphere (IPCC, 2005). In the portfolio of climate change mitigation actions, CO_2 capture and storage (CCS) has been considered as one of the viable options for reducing, primarily large point-source, emissions of anthropogenic CO_2 into the atmosphere (IPCC, 2005). Compatibility of CCS systems with current energy infrastructures, together with its potential to reduce CO_2 emissions over the next century, explains the strong interest in this technology. In addition, while the published storage needs for stabilizing CO_2 concentration at a safe level vary over a wide range (220-2,200Gt CO_2), the IPCC report estimates that the technical potential for worldwide geologic storage alone is sufficient to cover the high end of the economic potential range (IPCC, 2005).

This thesis follows the style of *SPE Journal*.

Four lines of evidence suggest that the recent increase in atmospheric concentrations of CO_2 is largely from human activities. The nuclei of carbon atoms in CO_2 emitted by burning coal, oil, and natural gas (fossil fuels) differ in their characteristics from the nuclei of carbon atoms in CO_2 emitted under natural conditions (Keeling, 1960; Stuiver et al., 1984). It takes millions of years for coal, oil, and natural gas to be formed deep inside the Earth. The fraction of their nuclei that were once radioactive has long ago changed to non-radioactive carbon. The CO_2 emitted from natural sources on the Earth's surface retains a measurable quantity of radioactive material. As CO_2 has been emitted through fossil fuel combustion, the radioactive fraction of carbon in the atmosphere has decreased. Forty years ago scientists provided the first direct evidence that combustion of fossil fuels was causing a buildup of CO_2 and thereby diluting radioactive carbon in the atmosphere by measuring the decreasing fraction of radioactive carbon-14 captured in tree rings, each year between 1800 and 1950 (Stuiver et al., 1984; Francey et al., 1999).

Secondly, starting in the late 1950s, scientists have collected data through precise measurements of the total amount of CO_2 in the atmosphere both at Mauna Loa, Hawaii, and at the South Pole. Nowadays, many locations around the world are used to monitor CO_2. The data so far collected show that the levels of CO_2 have increased each year worldwide (Keeling, 1973, 1976, and 1978). Furthermore, these increases are consistent with other estimates of the rise of CO_2 emissions due to human activity over this period. Thirdly, ice buried below the surface of the Greenland and Antarctic ice caps contains bubbles of air that were trapped when the ice formed. Measurements from the youngest and most shallow segments of the ice cores, show increasing CO_2 concentrations. Layers with air from only a few decades ago produce CO_2 concentrations nearly identical to those that were measured directly in the atmosphere at the time the ice formed (Keeling, 1978; Francey et al., 1999;IPCC, 2001, 2002). The CO_2 content of the pre-industrial parts of the cores arelower by almost 25% than what is measured today and are relatively constant over a period of 10,000 years (Keeling, 1978; Francey et al., 1999; IPCC, 2001,2002).

The fourth line of evidence comes from the geographic pattern of CO_2 measured in air. Worldwide the CO_2 distribution is not the same. According to observation, the CO_2 measurement on the northern hemisphere is slightly more than in the southern hemisphere (Stuiver et al., 1984; IPCC, 2001, 2002). The difference arises because most of the human activities that produce CO_2 are in the north and it takes about a year for northern hemispheric emissions to circulate through the atmosphere and reach southern latitudes.

The human population's dependency on fossil fuels as a source of energy is strong and the transition to alternate renewable energy sources is not in the current foreseeable future. The United States is by far the leading contributor of CO_2 emissions to the atmosphere followed by the Former Soviet Union and China.

Growing concern about human-induced climate change is driving technology development aimed at slowing the buildup of greenhouse gases in the atmosphere. The Kyoto Protocol, the first attempt to reach global consensus on how and how much to reduce greenhouse gas emissions, described in length two key prospective solutions to the problem of balancing the carbon cycle: reduce emissions and/or sequester more carbon. Improved efficiency and increased use of alternative energy to reduce the use of fossil fuels almost certainly will be part of the solution. A second key prospect is to increase the storage of waste CO_2 in reservoirs other than the atmosphere. Potential reservoirs for sequestering CO_2 include the terrestrial biosphere (Seneviratne 2003), the oceans (Drange et al. 2001), mineralized forms at the Earth's surface (Lackner 2002), and the deep underground formations (Holloway 2001). Electric power plants and large-scale industrial process plants are ideal candidates for CO_2 sequestration because they are point-source emitters.

1.1.1 Disposal in Geologic Storage

Injection of power plant-generated CO_2 into deep sedimentary formations is one way to limit the buildup of greenhouse gases in the atmosphere. Potential targets for CO_2 injection include depleted oil and gas reservoirs, deep unmineable coal seams, and deep saline aquifers. Technology for injecting CO_2 has long been used in the oil and gas industry for enhanced oil recovery. In addition, a pilot study of CO_2 injection for enhanced methane recovery from deep coal seams has been underway since 1996 (Gale & Freund 2001). These technologies potentially can provide economic return while storing CO_2 in the subsurface for long times. Injection of CO_2 into depleted oil and gas reservoirs, in particular, is a reasonable first approach to CO_2 storage because the infrastructure is largely in place. However, the storage capacity may not be sufficient to meet long-term needs. The technology also exists for injecting CO_2 into deep saline aquifers and pilot projects are underway in the Sleipner West oil field of the North Sea (Gale et al. 2001), the West Pearl Micro-pilot in New Mexico (Pawar et al., 2004), and the Frio Pilot Project in Texas.

The overall task of diverting power plant CO_2 to deep geologic reservoirs requires three steps: Capturing the flue gas, transport and injection of the CO_2, and sequestration of CO_2 in the reservoir. The present work focuses on the last step, CO_2 sequestration, in a saline aquifer. CO_2 is less dense than formation fluids. Once injected, some CO_2 dissolves into the pore water. The remainder rises buoyantly as a separate phase such that escape of CO_2 to the surface is a concern. Escape of CO_2 would compromise the objectives of injection and also could compromise safety, for example by contaminating shallow potable aquifers (Saripalli & McGrail 2002; Klusman 2003). Safe, long- term storage requires that the CO_2 be immobilized or otherwise prevented from migrating upward. Closed structures immobilize buoyancy-driven flow in oil and gas reservoirs and demonstrably have retained oil, natural gas, and naturally occurring CO_2 in the subsurface for millions of years (Pearce et al. 1996). As reported by Allis et al. (2001),

despite the abundance of CO_2 reservoirs in the Colorado Plateau- Southern Rocky Mountains region, no hazards from surface CO_2 accumulations are known. CO_2 injected into deep coal seams is immobilized by absorption onto the coal itself. Given a low permeability cap rock, deep saline aquifers theoretically can trap CO_2 hydrodynamically by slow moving, downward-directed formation waters (Bachu et al. 1994), by solubility in the pore waters (Weir et al. 1995), and by reactions with minerals and pore waters that convert CO_2 to carbonate minerals (Gunter et al. 1993). These hydrodynamic and geochemical trapping mechanisms may eliminate the need for geometric traps to retain CO_2 in deep saline aquifers.

1.1.2 Why Saline Aquifers

Deep saline aquifers provide no economic return for CO_2 injection, but they are widespread, are geographically associated with fossil fuel sources, and, because it is not necessary to identify and inject directly into closed structural traps, are likely to have large storage volumes and suitable injection sites in close proximity to power-plant sources of CO_2 (Bachu, 2003).

Deep aquifers potentially have CO_2-storage capacities sufficient to hold many decades worth of CO_2 emissions, but estimates of global capacity are poorly constrained, varying from 300 to 10,000 Gigatons CO_2 (Holloway 2001). In the United States, deep saline aquifers have a larger potential storage capacity than any other type of sedimentary formation, with estimates as high as 500 Gt of CO_2 storage (Bergman and Winter, 1995). The variation in estimates of storage capacity reflects different assumptions about the effectiveness of trapping mechanisms. The low estimate counts only CO_2 that could be stored as an immiscible phase in closed structures within aquifers. The high number assumes closed structures are not necessary and that CO_2 can be stored through a combination of hydrodynamic, solubility, and mineral trapping.

1.1.3 Mechanisms of Aquifer Storage of CO_2

Carbon dioxide is retained in geologic formations in different ways (Hitchon, 1996). First, CO_2 can be trapped as a gas or supercritical fluid under a low permeability caprock. This process, commonly called structural trapping. CO_2 could also be trapped within the pore spaces of the rock as the residual gas. CO_2 can dissolve into the groundwater, referred to as a solubility trapping. Furthermore, CO_2 can react directly or indirectly with minerals in the geologic formation leading to the precipitation of secondary carbonate minerals referred as mineral trapping. We'll describe residual, solubility and mineral trapping in the following sections.

1.1.3.1 Residual Trapping

Residual trapping refers to storage of free CO_2 in the pore spaces of sedimentary layers and the transport of that CO_2 away from the surface by regional groundwater flow (Bachu et al.1994). Free CO_2 is the main form of storage during injection, which can last 30-50 years. The injected CO2 is subject to injection-related hydrodynamic gradients and to buoyancy forces that cause it to form a plume that rises and spreads laterally until it meets a confining layer that impedes vertical ascent, causing the CO_2 to accumulate as a cap. The buoyant force of the CO_2 cap will depend on the difference in density between the CO_2 and the brine and on the dip of the confining layer. Provided a near horizontal confining layer and relatively small density difference, the CO_2 will travel with the downward-directed regional groundwater flow (Bachu et al. 1994), unless faults or other high permeability zones in the stratigraphic seal provide escape routes to the surface. The over-pressuring required for reasonable rates of CO_2 injection and buoyancy forces exerted by the CO_2 cap can widen small fractures, exacerbating the risk for CO_2 escape (Saripalli and McGrail 2002; Klusman 2003).

CO_2 can exist in three different states under the pressure and temperature conditions of deep saline aquifers: liquid, gas, and supercritical. Supercritical CO_2 behaves like a gas,

filling all the volume available, but has a density that varies with pressure and temperature from less than 200 kg/m3 to more than 900 kg/m3 (Angus et al. 1976). To reduce costs associated with injection and to limit the buoyancy forces and maximize the mass of free CO_2 that can fill a given pore volume, CO_2 should be injected in a supercritical state (Bachu, 2002). Early studies assumed an average surface temperature of 10°C, a geothermal gradient of 25°C/km, and a hydrostatic pressure gradient of 10 MPa/km to determine the depth at which the critical point for CO_2 (31.1 °C and 7.38 MPa) is reached (Holloway and Savage 1993). These studies set 800 m as a minimum depth for the confining layer. A depth corresponding to a pressure of 10-20 MPa, on the order of 1000 m, may be better because it avoids large CO_2 density gradients in the vicinity of the critical point (Holloway 2001).

In reality, the depths in the earth at which the pressure and temperature conditions for supercritical CO_2 are reached vary depending on climate conditions and the geology of the basin. In warm, over-pressured basins, the critical point can lie as shallow as 400 meters and the pressure-temperature distribution can be such that CO_2 passes with depth directly from a gas to a supercritical state. In cold basins, the depth at which the pressure and temperature conditions of the critical point are reached is likely to be deeper than the gas-to-liquid phase change. All things being equal, old, cold, stable basins are better for hydrodynamic trapping of CO_2 because higher CO_2 densities are reached at shallower depths and gradients in the density of CO_2 are more easily avoided (Bachu 2000). Old foreland and continental basins are best suited for hydrodynamic trapping because they tend to be cold, stable, and close to hydrostatic pressure, and to have erosion- or topography-driven, down-dipdirected regional flow regimes (Bachu 2000).

At 10 MPa and 35°C, CO_2 has a density of approximately 700 kg/m3. Under these conditions, a cubic meter of sandstone with 10% porosity contains approximately 70 kg of CO_2 if the pore space is completely filled by CO_2. However, saturation of CO_2 is not complete, some brine remains in the invaded pore spaces (Pruess et al. 2003; Saripalli &

McGrail 2002). In addition, nonuniform flow of CO_2 bypasses parts of the aquifer entirely. Darcy-flow based analytical and numerical solutions are used to evaluate some of these effects by simulating the advance of the CO_2 front over timescales of decades to hundreds of years and over distances of tens to hundreds of kilometers. To account for the extreme changes in density and viscosity of CO_2 with pressure and temperature, these models must incorporate experimentally constrained equations of state (Adams and Bachu 2002).

Initially the free CO_2 is distributed in radially decreasing concentrations in zones around the injection site (van der Meer 1996). Nearest the injection site lies a zone of near completely saturated pores, containing isolated beads of trapped brine, some of which evaporate into the CO_2 (Pruess et al. 2003). The middle zone contains mixed brine and CO_2 (Pruess et al. 2003; Saripalli & McGrail. 2002). In the outer zone, CO_2 is present only as aqueous species.

Following injection, CO_2 saturations around the injection site are predicted to decrease over tens of years as the free CO_2 rises buoyantly, spreads laterally, and dissolves into the brine (Weir et al. 1995). Over timescales of hundreds of years dispersion, diffusion, and dissolution can reduce the concentration of both free and aqueous CO_2 to near zero.

Pruess et al. (2003) used the Darcy-flow based Buckley-Leverette two-phase displacement theory to solve analytically the average saturation of injected CO_2 under a range of conditions. Under Buckley-Leverette conditions, the radius of the region swept by the CO_2 front increases with duration of injection and the CO_2 saturation decreases along that radius, but the average CO_2 saturation in the region is time independent. ssuming a homogeneous aquifer and uniformly swept region, Pruess et al. (2003) found that average saturation is most sensitive to permeability and for a range of rock types calculated a saturation range of 20-40%, with higher average saturations corresponding to rocks with higher permeabilities. Under these conditions, a rock with 10% porosity

has a storage capacity of 14-28 kg of CO_2 per cubic meter. These maximum values ignore flow patterns that may cause the CO_2 to bypass large parts of the aquifer. For example, taking into account buoyancy effects, Van der Meer (1995) estimated only 6% average saturation by CO_2. In addition, over certain ranges of viscosity ratio and injection velocity, the displacement front between CO_2 and brine can develop fractal fingers, rather than advancing as straight front as modeled by Darcy-flow. Fractal fingers may reduce the CO_2 volume of the aquifer accessed by CO_2 to as low as 1%. Formation heterogeneity, including low permeability layers and lateral discontinuities in permeable rock types can compartmentalize the aquifer vertically and laterally, reducing the amount of the aquifer accessible to the flow of CO_2. However, aquifer compartmentalization can also work in the other direction, limiting buoyancy and fingering effects and increasing the access of CO_2 (Johnson et al. 2001). Any aquifer bypassing that does occur, due either to buoyancy effects, fingering, or formation heterogeneity, may be partially compensated by higher saturations in the layers swept by CO_2 (Pruess et al. 2003).

1.1.3.2 Solubility Trapping

Solubility trapping refers to the CO_2 that dissolves into the brine. The CO_2- brine solution has a density greater than brine alone preventing buoyant flow of the CO2 toward the surface, even along high permeability vertical pathways such as faults Most models of solubility trapping assume instantaneous equilibrium between the brine and free CO_2. The solubility of CO_2 varies as a function of pressure, temperature, and salinity. Numerous models for CO_2 solubility in aqueous solutions have been published to describe this relationship, though few deal with high ionic strength, multicomponent brines.

Under typical cold deep-aquifer conditions of 10 MPa, 35°C, and 10% mass fraction salt, the solubility of CO_2 in brine is approximately 40 kg/m3 of brine. A rock layer with 10% porosity has a storage capacity of as much as 4 kg CO_2/m^3. Under the conditions of

interest for aquifer storage, CO_2 solubility increases approximately linearly by about 10 kg/m3 for each 10 MPa increase in pressure over the range of 10-30 MPa (Pruess et al. 2003). It decreases by an average of approximately 10 kg/m3 for each 25° C rise of temperature over the range of 35-100°C (Pruess et al. 2003). Thus under hydrostatic pressure gradients 10 MPa/km and average geothermal gradients of 25 °C/km the effects of increasing pressure and temperature with depth on the solubility of CO_2 essentially cancel each other out. However, around the injection site CO2 pressure increases to as much as twice hydrostatic pressure and CO_2 solubility increases with it. CO_2 solubility decreases by about 30% as salinity increases from zero to saturated NaCl (Moller et al. 1998, Pruess et al. 2003). CO_2 solubility is sensitive not only to the mass of salt dissolved (Bachu & Adams 2003), but also to the particular kind of salt. However, there are few experimental constraints on this effect. The extent to which CO_2 dissolves into the brine is influenced by the migration of the CO_2 front and by the rate of dispersion and diffusion of CO_2. Viscous fingering and buoyancy flow, which tend to limit the storage of free CO_2, may increase solubility trapping by increasing the surface area of the brine- CO_2 contact, allowing more rapid solution. In addition, diffusion of CO_2 into the brine can set up reverse density gradients that lead to convective mixing and increased rate of dissolution of free CO_2 (Lindeberg & Wessel-Berg 1997).

Through these processes, dissolved CO_2 becomes the dominant form of CO_2 storage in aquifers over periods of tens to hundreds of years following injection (Weir 1995). Over these timescales the CO_2 disperses (Law & Bachu 1996) by dispersion and diffusion, and dissolution into the brine (Lindeberg 1997). Continued migration and dispersion drive both free and dissolved CO_2 toward zero.

1.1.3.3 Mineral Trapping

Mineral trapping is the fixing of CO_2 in carbonate minerals due to geochemical reactions among aquifer brines, formation minerals, and aqueous species of CO_2. The density of CO_2 in calcite is 1250 kg/m3. In a rock with 10% porosity and the pores completely filled with calcite the storage capacity would be 220 kg CO_2/m3. However, the mass of CO_2 sequestered as carbonate minerals is sensitive to formation mineral and aquifer brine composition, pressure, temperature, and brine-rock ratio. Time is also important because mineral trapping reactions take hundreds to thousands of years and more to complete (Gunter et al. 1997).

Four kinds of models are available to simulate mineral-brine- CO_2 reactions: equilibrium, path of reaction, kinetic, and reactive transport models. Mineral equilibrium models and path of reaction models are used to calculate equilibrium solid phases and solution compositions for a given set of reactants based on a data set of equilibrium constants and activity coefficients. Equilibrium models calculate only the final state. Path of reactions models also calculate transitional phases along the way. These models do not provide information on the amount of time it takes to reach equilibrium or transition states. Kinetic models consider the rates of reactions. Widely available geochemical modeling codes such as PATHARC (Hitchon 1996), SOLMINEQ (Kharaka et al. 1988), and Geochemists Workbench (Bethke 1996) have been used for equilibrium, path of reaction, and kinetic simulations of CO_2 storage in aquifers. Because these models have no transport components, these studies simulate closed-system batch conditions and do not take into account migration of CO_2 through the aquifer (Gunter et al. 1993, 1996, 1997). Studies using full-scale reactive transport codes to simulate the flow, dissolution, and reaction of CO_2 are just becoming available (e.g. Johnson et al. 2001). In addition, experimental studies are investigating the kinetics of mineral-brine- CO_2 reactions in mineral separate and rocks to refine and test model reliability (Kaszuba et al. 2003; Liu et al. 2003). Early studies by Gunter et al. (1993) recognized three general cases for mineral-brine- CO_2 reactions: 1) reactions with mafic

minerals, including anorthite feldspar ($CaAlSi_2O_8$); 2) reactions with alkali feldspar (albite - $NaAlSi_3O_8$ and orthoclase – $KAlSi_3O_8$); and 3) reactions with carbonate minerals. They concluded that the most promising reactions for mineral trapping involve mafic minerals, which provide divalent cations (Fe^{2+}, Mg^{2+}, Ca^{2+}) for precipitation of carbonate. Mafic minerals such as olivine, pyroxene, and amphibole have the highest CO_2-fixing potential (Pruess et al. 2003), but are rare in sedimentary basins. The most common sedimentary-mineral sources of divalent cations are anorthite, mica-group minerals, especially glauconite, and clays, such that a general equation for mineral trapping in aquifers is:

Anorthite + Micas + Clays + CO_2 + H_2O ↔ Quartz + Kaolinite + Calcite + Dolomite + Siderite (1.1)

The mineral trapping takes place in three steps as demonstrated by the example of anorthite dissolution:

$CO_2(aq) + H_2O \leftrightarrow H+ + HCO_3$ (1.2)

$CaAl_2Si_2O_8 + 2H+ + H_2O \leftrightarrow Ca_2+ + Al_2Si_2O_5(OH)_4$ (1.3)

$Ca_2+ + HCO_3 \leftrightarrow CaCO_3 + H^+$ (1.4)

Which leads to the net reaction:

$CaAl_2Si_2O_8 + CO_2(aq) + 2H_2O \leftrightarrow CaCO_3 + Al_2Si_2O_5(OH)_4$ (1.5)

Anorthite Calcite Kaolinite

First the aqueous CO_2 dissociates in water, producing carbonic acid (Eq. 1.2); second the acid attacks the anorthite, leaching Ca^{2+} and neutralizing the acid (Eq. 1.3); and third, calcium carbonate precipitates (Eq. 1.4). Reactions with alkali feldspars do not provide

divalent cations for the precipitation of carbonate minerals and initially were thought to be of little significance for mineral trapping (Gunter et al. 1997). However, more recent work indicates that dissolution of alkali feldspars contributes to the fixing of CO_2 as the sodium alumino carbonate mineral dawsonite, $NaAlCO_3(OH)_2$ (Johnson et al. 2001, Saylor and Zerai, 2004, Zerai et al., 2005). In this case, the Na necessary for dawsonite precipitation is available in abundance in the brine, but dissolution of alkali feldspar provides a source of aluminum and neutralizes the acidic CO_2 according to (Johnson et al. 2001):

$$KAlSi_3O_8 + Na^+ + CO_2(aq) + 2H_2O \leftrightarrow NaAlCO_3(OH)_2 + 3SiO_2 + K^+ \quad (1.6)$$

The feasibility of mineral trapping of CO_2 in dawsonite is demonstrated by the Bowen-Gunnedah-Sydney Basin in Australia, which has abundant diagenetic dawsonite that formed in response to magmatic CO_2 (Baker et al. 1995). In addition, abundant dawsonite in the Green River Formation of Colorado and in Pleistocene ash beds at Olduvai Gorge Tanzania formed by reactions of aqueous carbonate species with nepheline in the sediment (Smith and Milton 1966).

Dissolution of carbonate minerals does not lead to mineral trapping of CO_2 (Gunter 1993). However, carbonate dissolution, and other mineral precipitationdissolution reactions can affect sequestration capacity by altering the permeability of the aquifer near the injection site.

1. 2 WATERFLOODING OPTIMIZATION

Fundamentally, waterflood involves pumping water through a well (injector) into the reservoir. The water is forced through the pore spaces and sweeps the oil towards the producing wells (producers). The percentage of water in the produced fluids steadily increases until the cost of removing and disposing of water exceeds the income from oil production. After this point, it becomes uneconomical to continue the operation and the waterflooding is stopped. Some wells remain economical at a watercut of up to 99%2. On the average, about one-third of the original oil in place (OOIP) is recovered, leaving two-thirds behind after secondary recovery. Other secondary recovery methods include CO_2 flooding and hydrocarbon gas injection, which requires a nearby source of inexpensive gas in sufficient volume.

Waterflooding is most often used as a secondary recovery method of increasing oil recovery in reservoirs where primary depletion energy has been exhausted. It is responsible for the high production rates in the U.S. and Canada3 where most of the fields are mature.

The number of new discoveries of significant oil fields per year is decreasing worldwide and most of the existing major oilfields are already at their mature stages. Consequently, it is becoming increasingly necessary to produce these fields as efficiently as possible in order to meet the global increase in demand for oil and gas (Sarma et al. 2005). For this reason, waterflooding projects are very commonly found in most of these mature fields. In many of these reservoirs however, water cuts from the production wells are very high and sometimes uneconomical thereby causing low ultimate recoveries (Arenas A. et al. 2003). This is because the injected water finds its way through conductive fractures and high permeability zones within the reservoir. Premature breakthrough mostly occurs in highly heterogeneous reservoirs. As a result, many water injectors do not usually achieve improved sweep efficiencies and a lot of the oil is by-passed. Various methods of solving the problem of poor sweep efficiency have been suggested. One method of

mitigating this problem is by employing smart production and injection wells (Brouwer D. R. et al. 2001, Glandt C. A. et al. 2003).

The best production schemes for oil and gas fields is being continually sought after in order to maximize the production from these existing fields. The objective of reservoir simulation is to determine the best production design for a given field. This goal has been commonly achieved by trial and error method. The reservoir engineer is left to decide what parameters to change and how the changes are made to improve the results. This imposes a high level of subjectivity to the optimization process. In the past few decades, researches have been made to develop simulators that can be used to determine the best production schemes. This can be (Esmaiel, T. E. H. et al. 2005) conceptually achieved by combining the existing reservoir simulators with some numerical search algorithms. The problem of production optimization requires the maximization or minimization of some objective function g(x). In this optimization problem, the objective function to be maximized is the net present value or cumulative oil production. Here, x is a set of controls, which may include bottom hole pressures, flow rates, choke size, etc and these controls may be manipulated in order to achieve an optimum value at which the objective function is maximized (or minimized). Optimization processes result in the improvement of future performance of a reservoir and therefore requires a simulation model of the real reservoir on which the optimization is carried out. The simulation model is a dynamic model that relates the objective function to the set of controls. The controls, x are also subject to other constraints such as surface production facilities, choke sizes, fracture limits, minimum allowable bottom hole pressures, etc and these constraints determine feasible values of the controls. These additional constraints pose major problems and further complicate the solution of the optimization process.

Two major categories of optimization algorithms exist in literature (Sarma P. et al. 2005): gradient-based algorithms (Ramirez, W. F. et al. 1984, Fathi, Z. et al. 1984) and stochastic algorithms. Gradientbased algorithms require an efficient technique of

calculating the gradient of the objective function g(x) with respect to the controls x. The optimal control theory is one of the most popular gradient-based algorithms.

The total number of controls to be adjusted is the product of the number of controls to be updated in time (control steps) and the total number of wells in the reservoir model. The number of controls could be very large even for a simple reservoir model with a reasonable number of wells and control steps, making the gradient estimation a very tedious process. Also, another major drawback of the gradient-based method using adjoint equations is that it requires explicit knowledge of the simulation model equations used to describe the dynamic system.

On the other hand, the stochastic algorithms such as genetic algorithms (Tavakkolian, M. et al. 2004) and simulated annealing (Zhou, C. et al. 1992) require many forward model evaluations but are capable of finding a global optimum with a sufficiently large number of simulation runs. Unlike the gradient-based algorithms, they do not require gradient estimations since the relationship between the objective function and the controls can be obtained from several forward models. However, the methods can be inefficient when the number of variables is large.

Production optimization problems involving reservoir modeling with time was first attempted by Lee and Aronofsky . The purpose of their study was to apply linear programming procedure to oil production scheduling problems. The problem was to determine an oil production schedule from 5 different wells that will give the maximum profit over an eight-year period. The constraints placed on the individual reservoir production rates of the wells included well pressures and pipeline capacity. They solved this problem using constant well interference coefficients as a substitute for a real reservoir simulation model. Wattenbarger , along with some other researchers extended this study further with the use of real reservoir simulation models for estimating the well

interference coefficients. Wattenbarger developed a method for maximizing withdrawals from a natural gas storage reservoir.

Natural gas is commonly stored in underground reservoirs during the summer months and then produced during the winter to meet seasonal demands. This seasonal production can be maximized through optimal scheduling of the individual wells. Wattenbarger proposed a method for optimizing the withdrawal schedule problem using the linear programming format. In his case, the withdrawal schedule was optimized in the sense that no discretized withdrawal schedule can be specified for the finite difference model that will give greater total seasonal production while still meeting the constraints placed on the problem. One of the constraints of this problem requires that the wellbore pressure of each well not fall below a minimum value. Also, the total reservoir withdrawal rate at any time is limited to the demand rates.

All the work previously mentioned have been limited by the number of phases, the phase behavior or by the geometry and size of the reservoir model. An approach, which uses only the control variables explicitly for numerical optimization has been developed. He was involved in the study of optimal control in water flood reservoirs using reservoir simulation models. He developed a method for numerical optimization of the net present value of a natural water drive and water drive by injection. The method uses an areal two-phase reservoir simulator to calculate the net present value (NPV) of a waterflooding scheme. In his study, the variables subject to control were the well rates. The waterflooding scheme that maximized the net present value was numerically obtained by combining reservoir simulation with control theory practices of implicit differentiation. He was able to achieve improved sweep efficiency and delayed water breakthrough by dynamic control of the well flow rates. For the reservoir models he considered, there was a net present value improvement of up to 11%.

Brouwer and Jansen studied the optimization of water flooding with fully penetrating, smart horizontal wells in 2-dimensional reservoirs with simple, large-scale heterogeneities. They used optimal control theory as an optimization algorithm for valve settings in smart wells. The objective was to maximize the recovery or net present value of the waterflooding process over a period of time. In the study, they investigated the static optimization of waterflooding with smart wells. Static implies that the injection and production rates in the wells were kept constant during the displacement process, until water breakthrough occurred. They observed significant improvements from simple reservoir models. They however, observed that more improvements could be achieved by dynamic optimization of the production and injections. In a later study (Brouwer D. R. et al. 2002), they addressed this same problem using dynamic optimization in which case, the inflow control valves in the wells were allowed to vary during the waterflooding process. Waterflood was improved by changing the well profiles according to some simple algorithm that move flow paths away from the high permeability zones in order to delay water break-through. This was achieved by calculating the productivity index (PI) for each segment. For each well, the segments with the higher PI are shut-in and the rates are equally distributed among the other segments that are open in order to maintain the production rates. They repeated this process until the optimum flow profile is obtained. This optimum flow profile was found to occur when the ultimate oil recovery from a successive step is lower than that obtained with the preceding flow profile.

Brouwer and Jansen investigated the optimization problem under two different scenarios of well operating conditions – purely pressure constrained and purely rate-constrained operating environments. They concluded that the benefit of smart wells under pressure-constrained operating conditions was mainly the reduced amount of water production rather than increased oil production. On the other hand, wells operating under rate constraints gave an increased production and ultimate recovery as well as reduced water production. Their results show that water breakthrough is delayed from 253 days for the

base case to 658 days for the optimized case Lorentzen et al. also carried out a study on the dynamic optimization of waterflooding using a different approach from those described above. He carried out his optimization by controlling the chokes to maximize cumulative oil production or net present value. Their new approach uses the ensemble Kalman filter as an optimization routine. The ensemble Kalman filter was originally used for estimation of state variables but has been adapted to optimization in their work. In their optimization study, they demonstrated the use of the ensemble Kalman filter as an optimization routine on a simple 5-layer reservoir with different permeabilities.

The above methodology provided by Lorentzen et al. avoids the use of the optimal control theory since no adjoint equations were needed and the model equations are treated as a "black box". This methodology avoids one obvious disadvantage of the optimal control approach when used as a solution to optimization problems – it entails the construction and solution of an adjoint set of equations. These adjoint equations require an explicit knowledge of the reservoir model equations and also require extensive programming in order to implement them. This has been shown by Sarma and Aziz.

CHAPTER II

PROBLEM FORMULATION

Because of its lower density, the injected CO_2 predominantly moves upward until it reaches, and accumulates under, impermeable layers. During this upward movement, CO_2 comes to contact with the resident brine triggering the dissolution trapping mechanism. The injected CO_2 forms a migrating plume. At the leading edge of the plume, CO_2 (non-wetting phase) displaces the brine (wetting phase) in a drainage process while at its tail water displaces CO_2 in an imbibitions process. The imbibition process, due to capillary forces, results in trapping of the CO_2 as an immobile phase in the pore spaces. Juanes et al. (2006) studied the hysteresis effect of saturation dependent relative permeability curves and concluded that it can have a significant contribution in CO_2 storage. Since aquifers are typically heterogeneous and anisotropic migration of CO_2 plume, and hence the amount of brine that comes to contact with it, depends on the distribution of aquifer hydraulic properties. Therefore, the CO_2 trapped via solubility and residual trapping mechanisms depend on the flow property distribution in the aquifer. In addition, pore size distribution in different regions of an aquifer affects the distribution of residual trapping in different parts. Hence, the spatial variability in the reservoir hydraulic properties is quite important in the design of CO_2 injection scenario.

It is possible to maximize the sweep efficiency and storage capacity of CO_2 in geologic formations by a controlled injection scenario. The current methods used in waterflooding optimization of oil reservoirs are NPV maximization (Brouwer et al., 2004; Sarma et al., 2006) and streamline-based time-of-flight optimization (Alhuthali et al., 2007). When optimization of NPV is considered, the injection and production scenario is systematically adjusted to find a scheme that produces the maximum asset value for a given time interval. When arrival time optimization is used, the goal is to obtain a uniform sweep efficiency by equalizing the arrival time of the injected phase. An

important difficulty in calculation of arrival times in streamline simulation is the difficulties that arise in calculation of streamline for compressible compositional runs (such as modeling CO_2 displacement). The method proposed in this paper is quite general and can be applied to both waterflooding optimization as well as CO_2 sequestration. We demonstrate the effectiveness of the proposed method by applying it to waterflooding and geologic CO_2 sequestration examples following our discussion of problem formulation.

2.1 OBJECTIVE FUNCTION

The objective of our optimization algorithm is to improve sweep efficiency of the injected CO_2 into heterogeneous saline aquifers, which in turn results in improve solubility and residual trapping. We achieve this objective by controlling the CO_2 injection rates in a manner that, despite the existing heterogeneities and preferential flowpaths, CO_2 movement in the reservoir is more uniform. In waterflooding of reservoirs, controllable dynamic well variables (such as bottomhole pressure, injection and production rates) are adjusted to optimize the performance of the field. Field performance (or the objective function of the optimization) can be formulated in terms of the response of the reservoir to input controls. A popular objective function is the economic profitability of the reservoir asset and is defined as its net present value, which is a function of the volume of injected and produced water, volume of produced oil, and other capital and operating costs. While cost is certainly an important consideration in geologic CO_2 storage, our goal in this paper is to focus mainly on maximizing CO_2 trapping by enhancing solubility and residual trapping mechanisms. To this end, we maximize the CO_2 spread in the aquifer by controlling the injection rate allocation.

Flooding rate allocation is a strong function of the spatial distribution of reservoir flow properties. A uniform water rate allocation usually results in different water breakthrough times at different producers. Upon water breakthrough at a production well the water injected at the injection point is continuously produced until the production

well is economically non-profitable. In addition, production of the injected water by wells that experience earlier breakthrough results in additional operating (recycling) costs that can be reduced if water breakthrough is delayed. One suitable objective function to avoid early water breakthrough can be obtained by trying to equalize and delay water production at relevant production wells despite the existing reservoir heterogeneity in the field. Therefore, by optimally distributing the injected water (through injection rate control), water production rate at different production wells can be equalized and delayed. This objective leads to a more uniform sweep efficiency and more extensive sweep of the reservoir for a fixed amount of injected water. Therefore, in our formulation we define an objective function that achieves: i) uniform sweep, and ii) delayed breakthrough.

Uniform sweep efficiency is obtained by minimizing a term in the objective function that penalizes the difference between water production rate at different producers. In addition, a second term is introduced to delay the water breakthrough. Figure 2.1 illustrates the two components of the objective function. Figure 2.1a shows well watercut curves for different producers with different breakthrough times t_b^1, t_b^2, t_b^3, and t_b^4 Figure 2.1b shows the effect of minimizing water breakthrough differences at different production well. A uniform sweep, however, can occur early or late in the life of the reservoir. Since a later breakthrough (under constant total water injection) implies a better sweep efficiency, it is desirable to delay water production by including a term that minimizes field water production. Mathematically, the objective function is now expressed with two terms as follows:

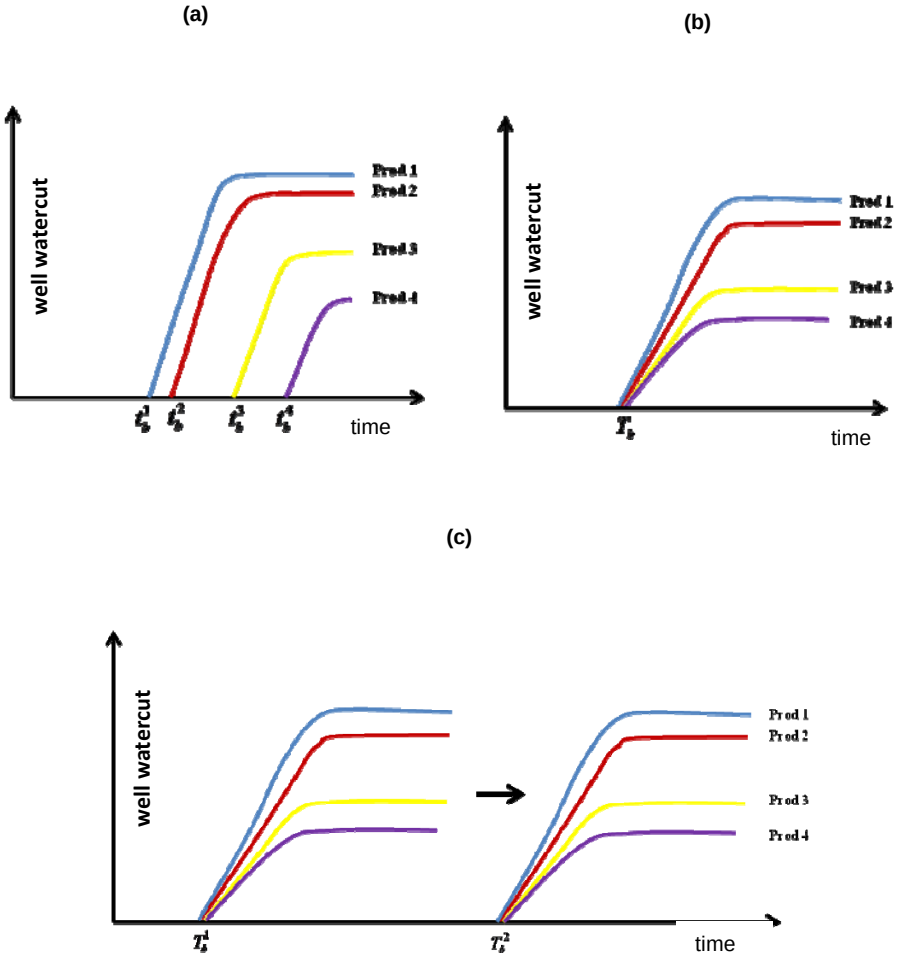

Fig. 2.1- (a) Well watercut in a base case with uniform injection and production scenario where producers have different breakthrough times; (b) Well watercut curves for an optimized case in which uniform sweep is achieved and producers experience the same breakthrough time; (c) Well watercut curves for an optimized case in which the sweep efficiency is maximized and field water production is minimized, with the former resulting in equalized breakthrough times at all wells and the latter delaying the breakthrough time.

$$J_1(\mathbf{u}) = \sum_{t=1}^{T_{sim}} F_t \sum_{\substack{i,j \\ i \neq j}}^{N_w} \left(q_i^{wprod}(\mathbf{u}) - q_j^{wprod}(\mathbf{u}) \right)^2 + \sum_{t=1}^{T_{sim}} G_t \sum_{i}^{N_w} q_i^{wprod}(\mathbf{u}) \tag{2.1}$$

where t denotes the report times at which the objective function is calculated and T_{sim} represents the total simulation time. The total number of producers is denoted with N_w and the rate of water production at producer i is represented with q_i^{wprod}. The decision variable of the optimization problem is denoted with the control vector $\mathbf{u}$, which in our examples consists of water injection rates q_i^{winj} and total fluid production rates q_i^{tprod}. The weight functions F_t and G_t are chosen to tune the contribution of the misfit terms and total field water production (i.e., the inner summation in the second term) at different time steps, respectively. Since we intend to delay water breakthrough, the weights are chosen to exponentially decrease in time. This choice for the weights places significantly more importance on having equal water production rates at earlier times and less emphasis on deviations from equal water production rates later after breakthrough happens.

As shown in Figure 2.1c, together the two terms of the objective function favor solutions that achieve a uniform and late water breakthrough at all wells. One could also include an additional term to favor solutions with lower overall cost (i.e., a higher NPV). In that case, the objective function will be of the form:

$$J(\mathbf{u}) = J_1(\mathbf{u}) - J_2(\mathbf{u}) \tag{2.2}$$

with

$$J_2(\mathbf{u}) = W \sum_{t=1}^{T_{sim}} \sum_{\substack{i,j \\ i \neq j}}^{N_w} \frac{\left(r_{oprod} q_i^{oprod}(\mathbf{u}) - r_{winj} q_i^{winj}(\mathbf{u}) - r_{wprod} q_i^{wprod}(\mathbf{u}) \right)}{\left(1 + r_{disc}\right)^{N_t}} \tag{2.3}$$

representing the NPV. In the above equation, the costs of injecting and producing a unit volume of water are shown with r_{winj} and r_{winj}, respectively, while the price per unit volume of oil is represented with r_{oprod}. The discount factor r_{disc} is used to account for the time value of money in computing the NPV. In this paper, however, we set $W = 0$ which effectively removes the NPV terms and optimizes the J_1 term of the objective function.

With the above objective function the optimization problem can be expressed as:

$$\begin{aligned} &\min_{\mathbf{u}\in\mathbf{U}} J(\mathbf{u}) \\ &s.t. \quad f_j(\mathbf{x},\mathbf{u}) = 0 \qquad j = 1,2,....N_f \\ &\qquad g_i(\mathbf{u}) = 0 \qquad i = 1,2,....N_g \\ &\qquad h_i(\mathbf{u}) \le 0 \qquad i = 1,2,....N_h \end{aligned} \tag{2.4}$$

where $f_i(\mathbf{x},\mathbf{u})$, $g_i(\mathbf{u})$, and $h_i(\mathbf{u})$ are the flow equations, equality, and inequality constraints (linear or nonlinear) on the control variable. Examples of field constraints are injection /production bottomhole pressure, total or group injection/production rates, as well as economic constraints such as maximum well watercut. Of particular importance in CO2 storage is to have a constraint that keeps the CO_2 injection pressure below the fracture pressure of the aquifer rock by limiting the injection rate. In the examples of this paper, we have used a total injection/production constraint for waterflooding example and total injection volume constraint for the CO_2 sequestration problem. The BFGS algorithm (Nocedal and Wright, 2006) is used to minimize the above objective function subject to the stated mass balance (flow) equations and total injection/production constraints.

In the first part of the objective function which is as follow we expect a general behavior as shown in Figure 2.2.

$$\sum_{t=1}^{T_{sim}} F_t \sum_{\substack{i,j \\ i\neq j}}^{N_w} \left(q_i^{wprod}(\mathbf{u}) - q_j^{wprod}(\mathbf{u}) \right)^2 \tag{2.5}$$

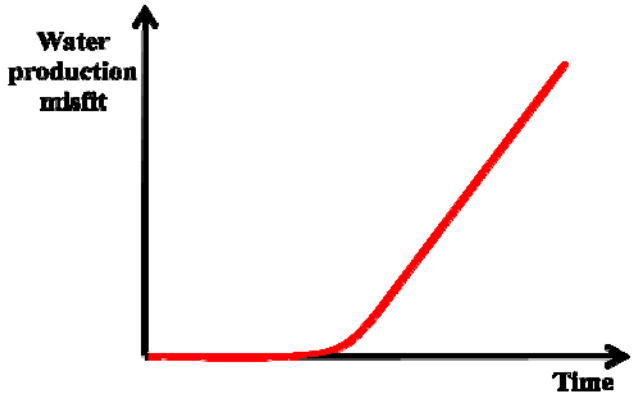

Fig. 2.2- Increasing behaivior of the objective function (water production misfit) over the time.

As you can see in the Figure 2.2 the misfit value has an increasing trend over the time and in the beginning the misfit is zero because in the beginning (before field breakthrough) non of the producers produce water. Therefore the objective function has higher values for later timesteps and this causes the optimization algorithm to focus on minimizing those values. The fact is that we want to have a uniform sweep efficiency which technically means that different producers will have the same breakthrough and for that we have to have higher weights on the misfit of water production in earlier timesteps.

One idea is to use an exponential weight function over the entire weight function. This weight function could be as below:

$$F_t = e^{-\frac{t}{\lambda}} \qquad \lambda \succ 1 \qquad 1 \le t \le T_{sim} \tag{2.6}$$

As we experienced this type of weight function is very sensitive to the value of λ meaning that for different values of λ we'll get different solutions which provide the production values which are totally different from each other. Therefore we introduce another weight function together with the above weight function. This weight function attempts to first equalize the values of the misfit over the time and then we can apply the exponential weight function. Equation 2.7 shows the final weight function that we have used:

$$F_t = \frac{1}{\Delta R_i} e^{-\frac{t_i}{\lambda}}$$
$$\lambda \succ 1 \qquad (2.7)$$
$$1 \le t_i \le T_{sim}$$

In which ΔR_i is the total misfit of water production rate over report time t.

The weights of misfit terms play the role of the coefficients of the objective function and these weights should be constant at different iterations for each term of the objective function. Moreover the report times that the objective function is calculated must be uniform and constant during all the iterations.

The other part of the objective function which is the field water production rate has the same behavior and we are applying the same type of the objective function for that.

CHAPTER III

APPLICATION OF THE METHOD IN WATERFLOODING OPTIMIZATION

Among the methods that have been using in waterflooding we can name NPV optimization and arrival time optimization. In NPV optimization the revenue is maximized based on the total oil and water production, oil price and water injection and production cost and discount rate as shown in equation 3.1.

$$NPV(\mathbf{u}) = W\sum_{t=1}^{T_{sim}}\sum_{i}^{N_w}\frac{\left(r_{oprod}q_i^{oprod}(\mathbf{u}) - r_{winj}q_i^{winj}(\mathbf{u}) - r_{wprod}q_i^{wprod}(\mathbf{u})\right)}{\left(1+r_{disc}\right)^{N_t}} \tag{3.1}$$

In the above equation, the costs of injecting and producing a unit volume of water are shown with r_{winj} and r_{winj}, respectively, while the price per unit volume of oil is represented with r_{oprod}. The discount factor r_{disc} is used to account for the time value of money in computing the NPV. While cost is certainly an important consideration in geologic CO_2 storage, our goal in this paper is to focus mainly on maximizing CO_2 trapping by enhancing solubility and residual trapping mechanisms. To this end, we maximize the CO_2 spread in the aquifer by controlling the injection rate allocation.

In arrival time optimization which uses streamline simulation, the arrival time of the particles (the time that it takes that a particle reaches to producer starting from injector) is maximized in an attempt to maximize sweep efficiency.

As we discussed in previous chapter in our method we try to minimize the misfit of water production rate among the producers to achieve uniform sweep. In this chapter we show the results of applying this objective function in waterflooding optimization for a

3D synthetic model and for PUNQ-S3 model. The same models will be used in case of CO_2 sequestration optimization.

3.1 SYNTHETIC 3D MODEL

The synthetic model is a 3D heterogeneous reservoir with three layers. Figure 3.1 shows the porosity and permeability distribution of the model. The locations of the injectors and producers are illustrated in Figure 3.2. The model contains a 13-spot well configuration with four injectors and nine producers.

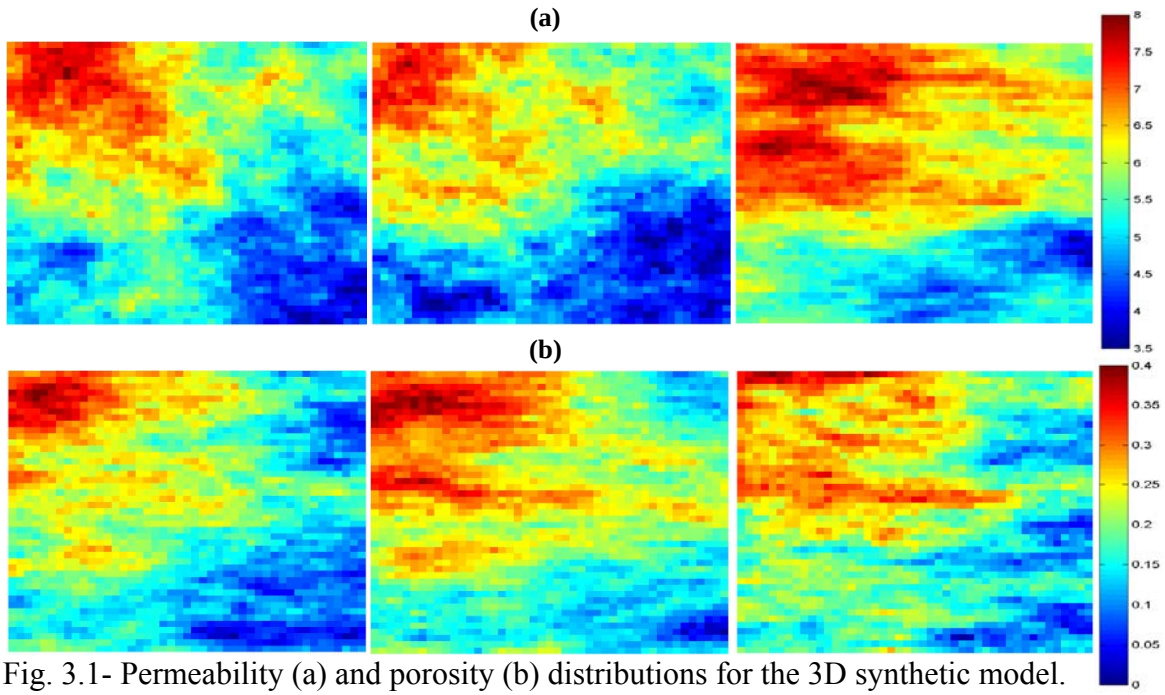

Fig. 3.1- Permeability (a) and porosity (b) distributions for the 3D synthetic model.

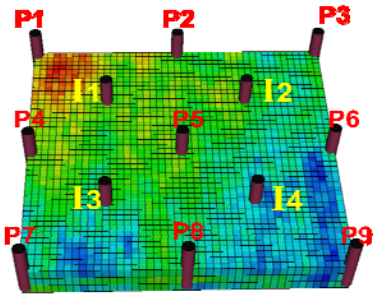

Fig. 3.2-Well configuration of the synthetic model.

In the following examples, we only minimize J_1 without considering the NPV term (J_2). A summary of the oil and water properties is reported in Table 3.1 while other simulation details are summarized in Table 3.2.

Table 3.1 PVT data for waterflooding examples

		P_{ref} (psi)	B (bbl/STB)	C (psi^{-1})	μ(cp)
Synthetic	Water	14.7	1.00	1.0e-5	1.00
	Oil	14.7	1.00	1.0e-5	2.00
PUNQ	Water	5863.8	1.04	3.3e-6	0.31
	Oil	2897.1	1.30500	3.44e-6	0.29

Table 3.2 Reservoir and fluid properties for waterflooding examples

Parameter	Synthetic	PUNQ-S3
Rock compressibility (psi^{-1})	8.10E-06 (at 5863.8psi)	3E-6 (at 14.7psi)
Datum depth (ft)	4000	2355
Datum pressure (psi)	5863.8	2000
OWC depth (ft)	4100	10000
GOC depth (ft)	---------	100
Oil density (lb/ft^3)	52.1	43.7
Water density (lb/ft^3)	63.29	62.43
Gas density (lb/ft^3)	0.0548	0.063
Reservoir dimensions	45 ×45×3	19 ×28×5
Total injection time	5000 days	5000 days
No. of injectors	4	4
No. of producers	9	4
No. of control timesteps	5	5
No. of control variables	65	40
Type of control	Inj. & prod. rate	Inj. & prod. rate
Total injection constraint	1 PV	1 PV

Figure 3.3 displays saturation-dependent oil and water relative permeability functions for this experiment.

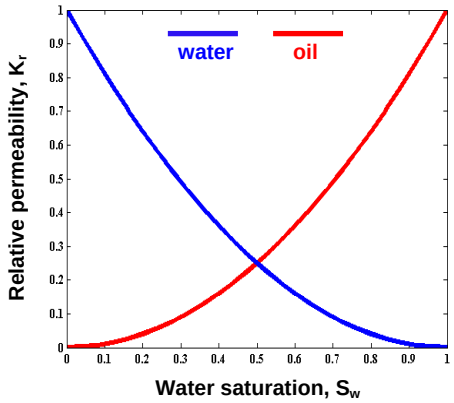

Fig.3. 3- Water and oil relative permeability as a function of water saturation.

Water saturation plots for the base and optimized cases after 30 and 36 months (end of simulation) are depicted in Figure 3.4. The improvement of the sweep efficiency in the optimized case over the base case is apparent. As discussed earlier a uniform sweep leads to producers having similar breakthrough times.

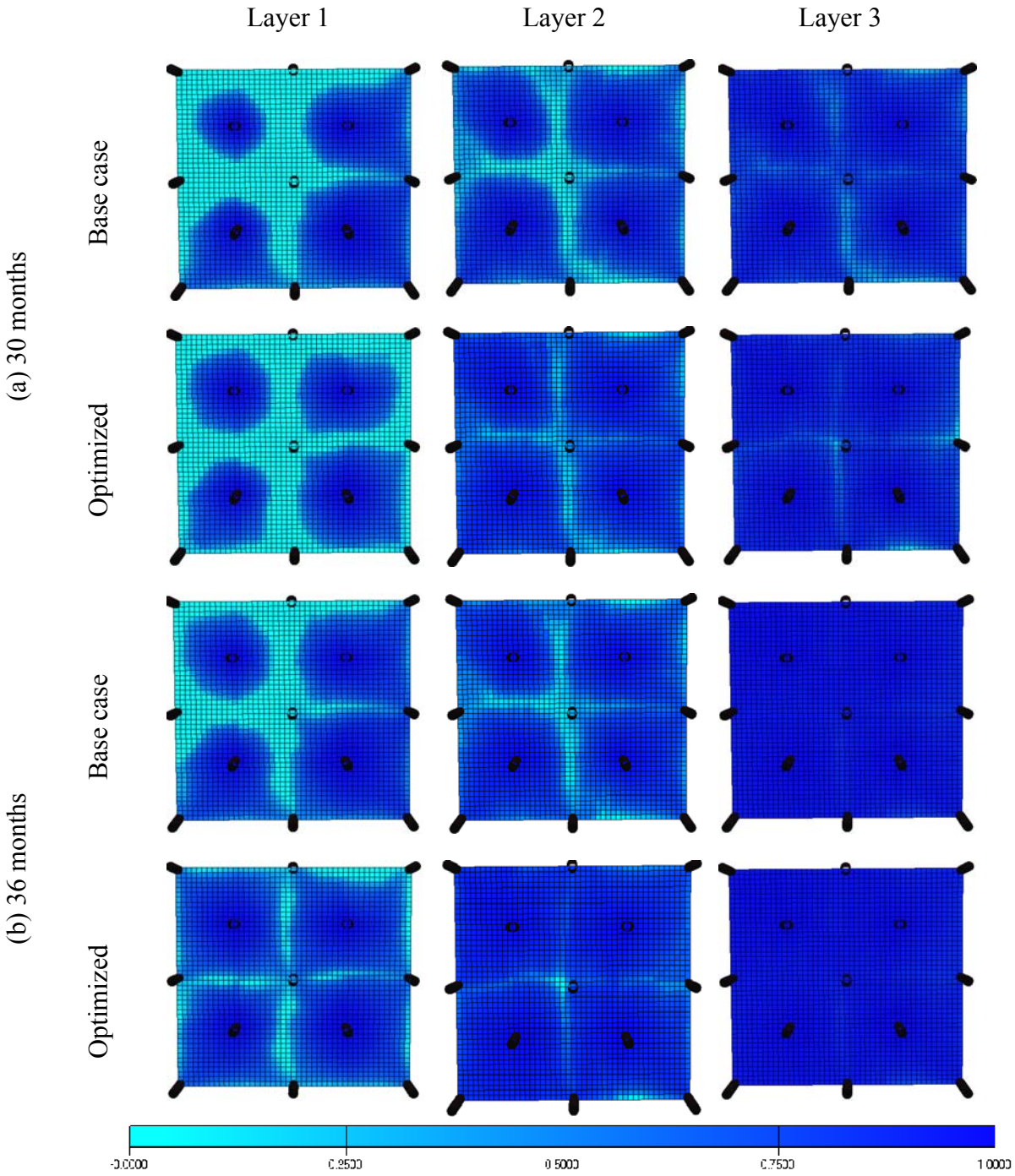

Fig. 3.4- Water saturation for the synthetic model after 30th (a) and 36th (b) months. In each case the results for the base case (top row) and optimized case (bottom row) are shown.

Figure 3.5a shows well watercut plots for the base case (corresponding to the initial solution of optimization) while Figure 3.5b display the same plots after optimized. The corresponding field watercut plots are shown in Figure 3.5c.

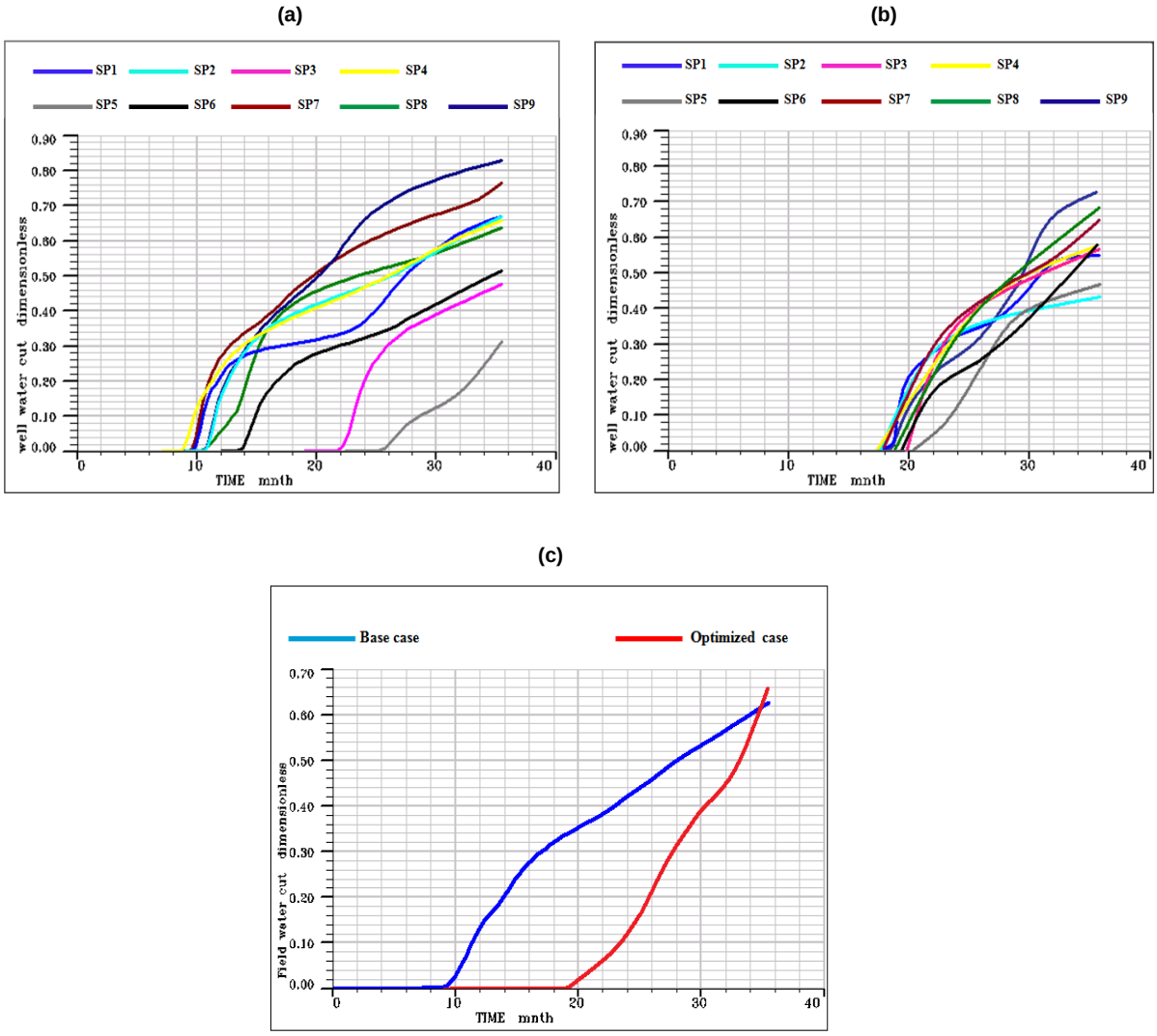

Fig. 3.5- Watercut curves for the synthetic model: Well watercut curves for the base case and the optimized case are shown in (a) and (b), respectively, while field watercut plots are shown in (c).

It is evident from these figures that the base case breakthrough times vary from less than 10 months to around 20 months. After optimization, however, all breakthrough times occur almost at the same time (20 months) indicating the effectiveness of the objective function in both equalizing and delaying breakthrough times. A similar behavior is observed in the field breakthrough time (Figure 3.5c). The effect of sweep efficiency optimization and delayed breakthrough time on the total oil and water productions is shown in Figure 3.6. Figure 3.6a shows the total (field) water production while Figure 3.6b displays the total (field) oil production for the base and optimized cases. The substantial decrease (increase) in the water (oil) production confirms the positive impact of the proposed objective function on overall recovery from the field.

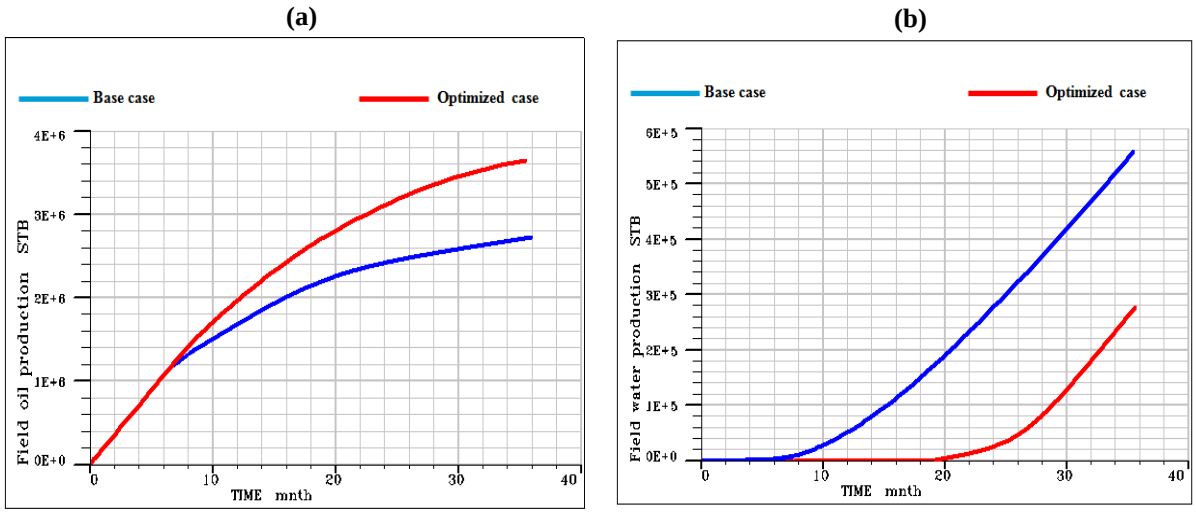

Fig. 3.6- Production plots for the base and optimized cases clearly show the advantage of optimization: total water and oil production plots are shown in (a) and (b), respectively.

3. 2 PUNQ-S3

Our second example is based on a waterflooding experiment in the PUNQ-S3 model, a 3D heterogeneous reservoir with five layers that was originally published in (see PUNQ-S3 website). A three-phase black-oil simulation with oil, water, and gas as existing phases is considered. Figure 3.7 illustrates the well configuration for the waterflooding. The permeability and porosity distributions for the all layers are shown in Figures 3.8a and 3.8b, respectively. When CO_2 sequestration is considered, the injectors are perforated only in the bottom most layer to increase CO_2 contact with resident brine during the density-driven upward movement of CO_2. To simulate an open boundary reservoir for CO_2 sequestration an aquifer is simulated on the boundary of the bottom most layer. The aquifer is chosen to be in the bottom layer to prevent its effect on trapping CO_2 since the gas moves to upper layers. The only role of the open aquifer is to prevent extreme pressure increases. Bulk injection of CO_2 into closed saline aquifers may results in pressure buildup that exceeds fracture pressure and can compromise the integrity of aquifer seal.

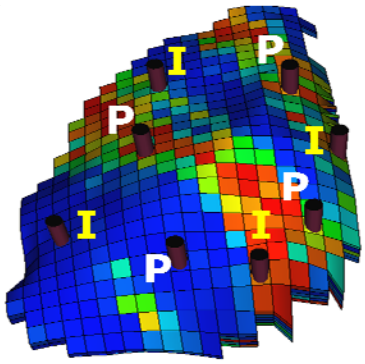

Fig. 3.7- Well configuration for the PUNQ model under waterflooding.

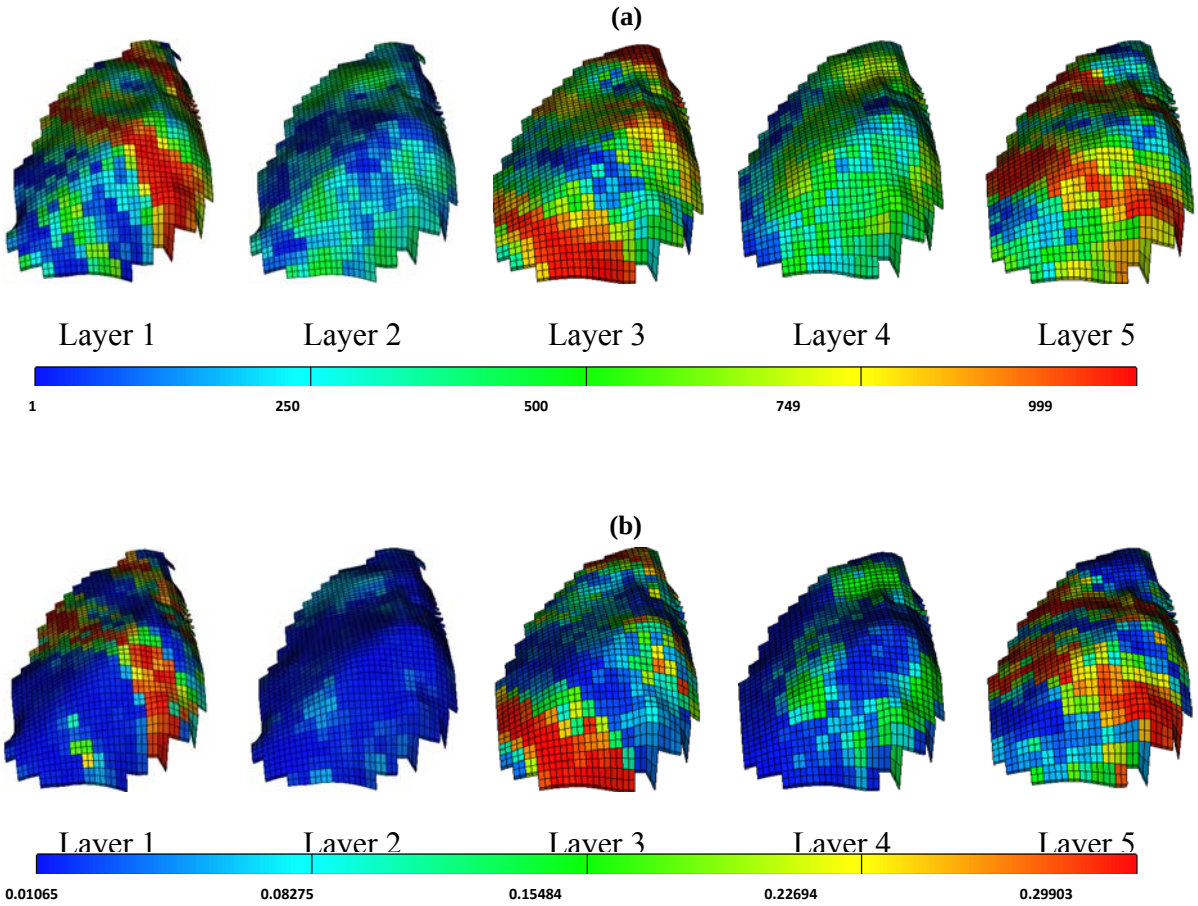

Fig. 3. 8- Permeability (a) and porosity (b) distributions for different layers of the PUNQ model.

For the PUNQ model, we minimize the objective function J_1 in Equation 2.1. Tables 3.1 and 3.2 contain the fluid properties and other simulation information for waterflooding experiment with the PUNQ and the 3D synthetic model.

Figure 3.9 presents the pressure-dependent formation volume factor and viscosity of the gas phase (3.9a and 3.9b, respectively). In Figure 3.9c the relative permeability curves for each phase are shown as a function of water saturation.

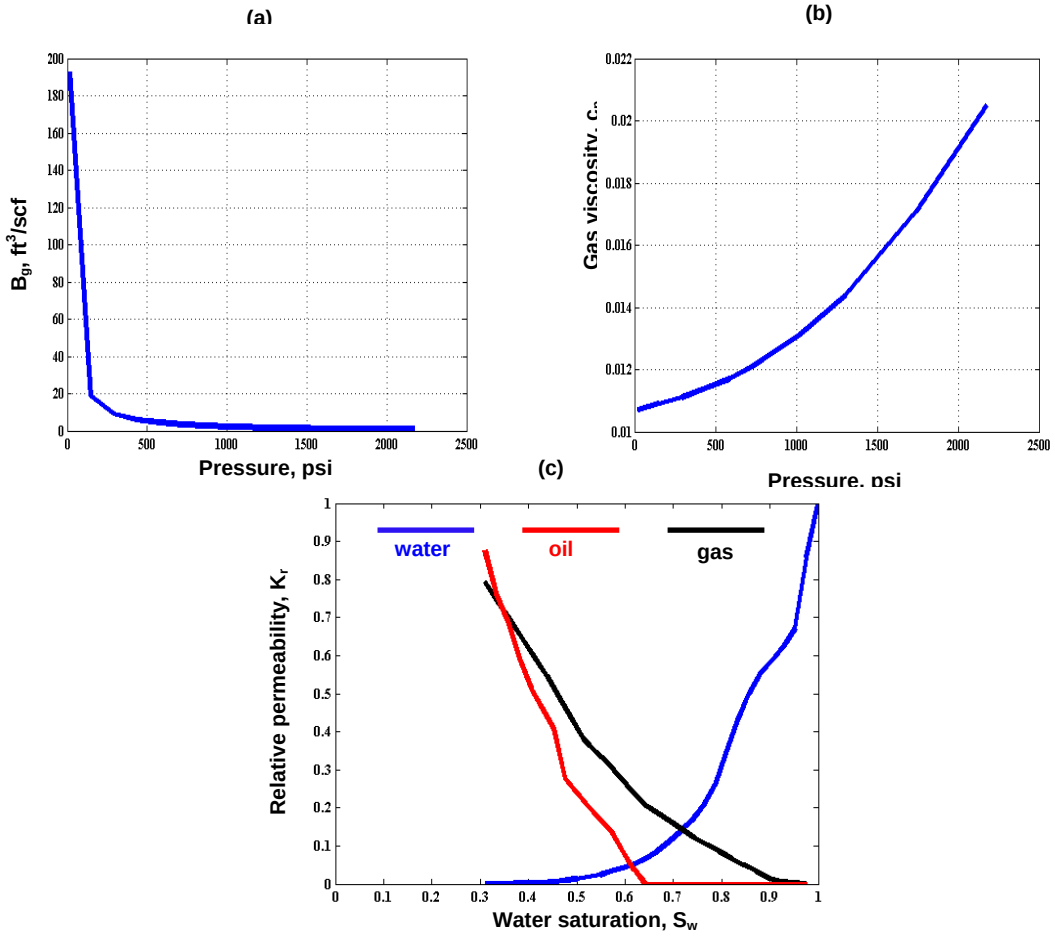

Fig. 3.9- Formation volume factor (a) and viscosity (b) of the gas phase as function of phase pressure for the PUNQ model under waterflooding. The water, oil, and gas relative permeabilities as a function of water saturation are displayed in (c).

The optimization results are displayed in Figures 3.10 through 3.12. Figure 3.10 shows the water saturation maps in all layers after 4000 (3.10a) and 5000 (3.10b) days.

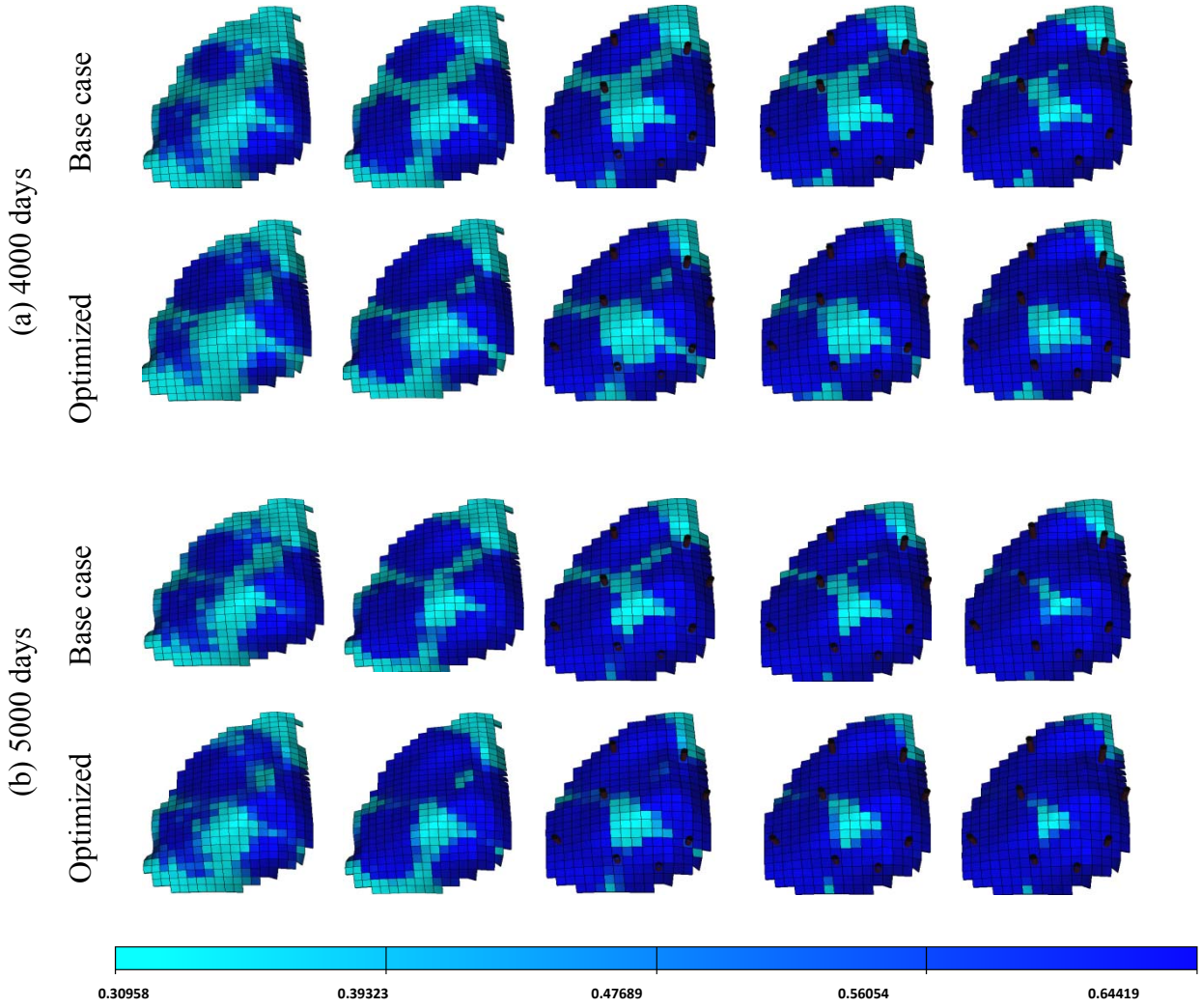

Fig. 3.10- Water saturation for the PUNQ model after 4000 (a) and 5000 (b) days. In each case the results for the base case (top row) and optimized case (bottom row) are shown. The sweep efficiency in optimized case is clearly improved relative to the base case.

The improvement in the case of maximized sweep efficiency is evident from a visual inspection of the results. Figure 3.11 confirms that the breakthrough happens almost at the same time for all the producers, implying that the injected water is uniformly distributed within the reservoir. In the optimized case, the field breakthrough is delayed

by more than 1000 days. The uniform and delayed breakthrough results in increased total oil production and reduced total water production as shown in Figure 3.12.

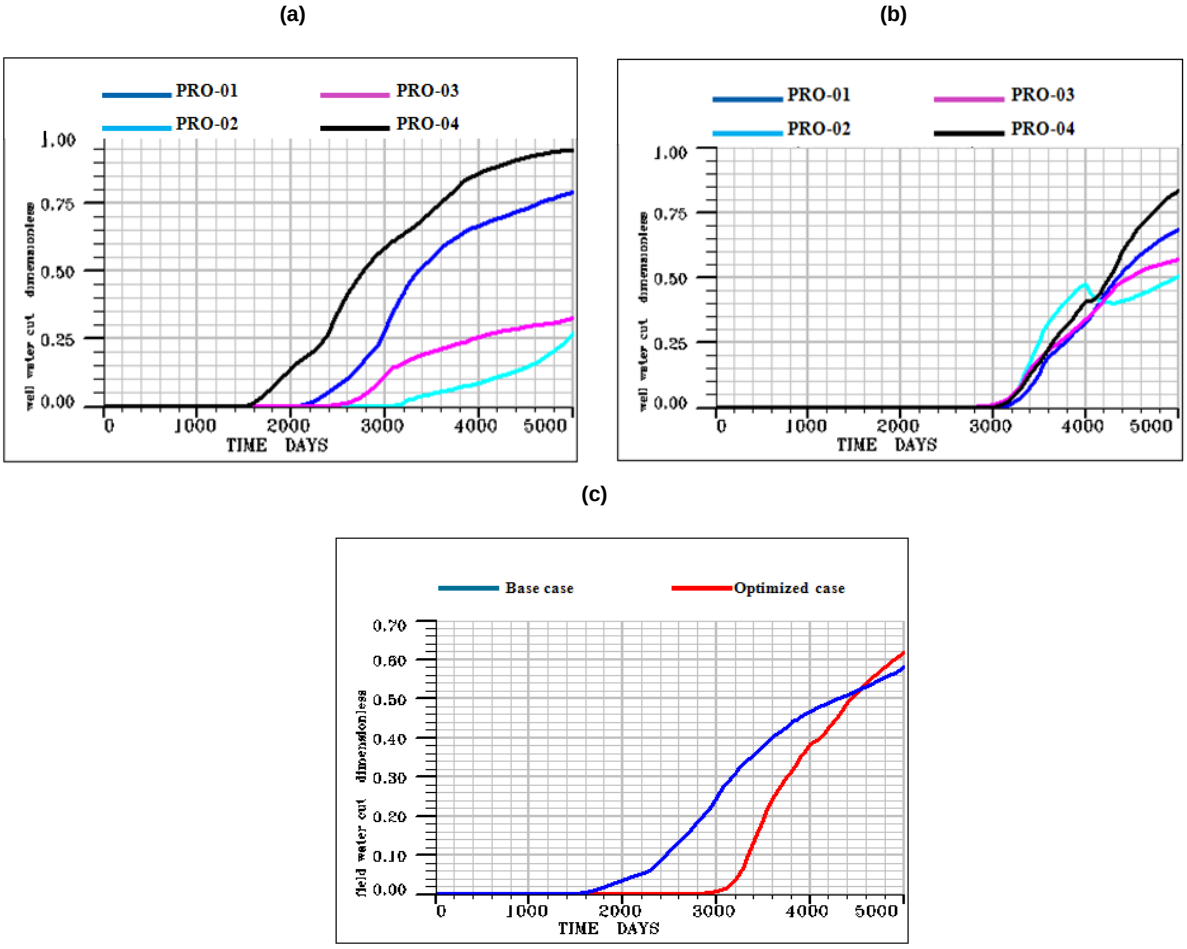

Fig. 3.11- Watercut curves for the PUNQ model: Well watercut plots for the base case and the optimized case are shown in (a) and (b), respectively, while field watercut curves are displayed in (c). The figures clearly illustrate that watercut occurs at almost the same time and at a delayed time 3000 days (compared to the base case of 1600 days).

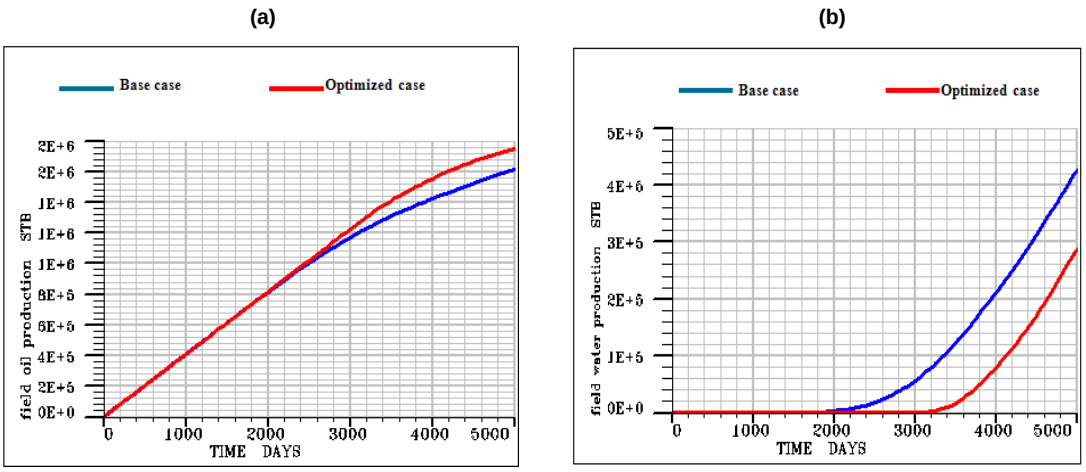

Fig.3.12- Production plots for the base and optimized cases illustrating the advantage of optimization: total oil (a) and water (b) production plots are shown.

As we saw in the above examples this new method of sweep efficiency optimization is capable of providing optimal trajectories which results in uniform sweep efficiency through minimizing the misfit of water production rate and delaying the field breakthrough. It must be mentioned that any type of constraints could be applied in the algorithm of the optimization including constraints on production quantities (water cut, water production rate, BHP etc) and the constraints on the controls (injections and production rates and BHPs).

In next chapter we will use the same algorithm to optimize the CO_2 storage into saline aquifers. Since in CO_2 sequestration no production happens we have to do some adjustments to be able to use the developed algorithm.

CHAPTER IV

APPLICATION OF THE METHOD IN CO_2 SEQUESTRATION OPTIMIZATION

The methods that have been recently proposed to accelerate CO_2 sequestration are based on brine injection (Keith et al., 2005; McMillan and Bryant, 2007; Leonenkoy and Keith, 2008; Hassanzadeh et al., 2009; Anchliya et al., 2010). The effect of simultaneous CO_2 and brine injection and also water-alternate-gas systems have been studied by several authors (Juanes et al., 2006; Sifuentes et al., 2009; Anchliya et al., 2010). These methods can affect both residual and solubility trapping. Introducing fresh brine into regions of the aquifer that are saturated with CO_2 increases the dissolution and residual trapping. Hassanzadeh et al. (2009) studied the effect of including brine injectors to accelerate the solubility mechanism. They showed that brine injection can potentially accelerate CO_2 dissolution in saline aquifers and therefore reduce the risk of CO_2 leakage. Leonenkoy et al. (2007) also suggested a top-hat model in which brine injection starts when CO_2 injection stops. The brine producers are placed far from the injectors to prevent production of CO_2-rich brine. A particularly important problem in improving CO_2 storage capacity in large scale heterogeneous field problems is allocating optimal injection rates based on the long term performance of the aquifer given the existing heterogeneity in hydraulic properties.

In this chapter we present the application of the developed method to improve sweep efficiency of the injected CO_2 into heterogeneous saline aquifers. The objective is to accelerate solubility and residual trapping by optimizing injection rate allocations based on the existing heterogeneity in the hydraulic aquifer properties and the intrinsic physical properties of the CO_2 sequestration problem. Aquifer heterogeneity exists in multiple scales, each with their respective uncertainty and influence on the flow and transport regime (IPCC, 2005). Heterogeneities can affect various aspects of the design and monitoring of permanent CO_2 storage in deep saline aquifers. Particularly important

in determining the global flow regime is the large scale structural continuity and layering of aquifer formation. Small-scale or local heterogeneity also plays an important role in CO_2 transport and trapping behavior (Bryant et al., 2006). It has been observed that as the heterogeneity of the aquifer increases, capillarity effects become more dominant during the buoyant CO_2 displacement, leading to enhanced dissolution and residual trapping (Bryant et al., 2006). These important properties of flow and transport in heterogeneous aquifers calls for an optimal well placement and injection rate allocation design to maximize the sweep efficiency of CO_2 and increase the storage capacity of aquifers. In this chapter, we study the rate allocation optimization problem and develop a new algorithm to improve the sweep efficiency of the injected CO_2.

The goal of our optimization formulation is to maximize permanent storage of CO_2 in heterogeneous geologic formations. The target trapping mechanisms in our study are dissolution and residual trapping, which we strive to achieve by adjusting injection rate allocations by accounting for aquifer heterogeneity. Since in CO_2 sequestration the main focus is on injecting CO_2 into the formation, there may not be any production wells in the field. Hence, our problem formulation that relies on the breakthrough curves need to be modified for application to CO_2 storage problems. We introduce the concept of the pseudo wells to apply our problem formulation to CO2 storage problems.

Pseudo production wells are producers with very small (negligible) total fluid production rate introduced in the flow simulation with the purpose of aiding the optimization processes. The production rates at these producers are chosen to be too small to have an influence on the overall flow regime. In our case, the producers are used to indicate the arrival of CO_2 (and its fractional production rate), which can be used to equalize production rates at all producers and to delay CO_2 breakthrough. Since the pseudo wells do not exist in the real reservoir, the user can have flexibility in choosing their location based on the objective of the project. Once pseudo wells are introduced, the proposed formulation can be easily applied to CO_2 storage problem. Similar to the waterflooding

problem, the objective here is also to maximize the sweep efficiency by mobilizing the injected CO_2 uniformly in all directions and exposing a larger volume of fresh brine to the CO_2 plume, leading to an enhanced solubility and residual trapping. As such, the problem formulation in Equations (2.1)-(2.4) remain unchanged (except for the pseudo wells replacing the production wells). We illustrate the effectiveness of the method by comparing this method with direct maximization of the stored gas. In this case the objective function will be defined as follow:

$$StoredGas = ResidualGas + DissolvedGas \tag{4.1}$$

Table 4.1 and 4.2 summarizes some optimization and simulation properties for the two models we use.

Table. 4.1- Reservoir and fluid properties for CO2 storage.

Parameter		**Value**	
Reservoir temperature		40 °C	
Rock compressibility		5e-5	
Datum pressure		89.2 atm	
Number of components		3	
Maximum residual gas saturation		0.4	
Residual water saturation		0.31	
Reference density of solid phase[1]		2650 kg/m^3	
	H2O	**CO2**	**NACL**
Total mole phase fraction	0.9	0.0	0.1
Water diffusion coefficients	0.0001	0.0001	0.0001
Gas diffusion coefficients	0.001	0.001	---------

Table. 4.2- General simulation information for CO2 storage.

Parameter	Synthetic	PUNQ
Reservoir dimensions	45 ×45×3	19 ×28×5
Total injection time	10 years	30 years
No. of injectors	4	4
No. of *pseudo*-producers	7	4
No. of control timesteps	5	5
No. of unknowns	20	20
Type of control	Injection	Injection
Total CO_2 injected (constraint)	0.61 PV	0.52 PV
Total brine extracted (constraint)	2.55e-4 PV	6.32e-6 PV
Total CO_2 extracted	0.0110 PV	0.0075 PV

4.1 SYNTHETIC 3D MODEL

The pseudo well configuration for this model is illustrated in Figure 4.1. We examine two different optimization methods. First, sweep efficiency optimization similar to the method used for waterflooding optimization. The second method directly optimizes the total stored CO_2 in the aquifer. In this study by free gas we mean the mobile gas which is neither dissolved nor trapped as residual gas. The optimization goal is to have the minimum free gas or in our case the maximum dissolved and residual gas. There are three cases that will be compared together. The base case is the initial solution for the optimization in which the total amount of injection is uniformly distributed between the injectors.

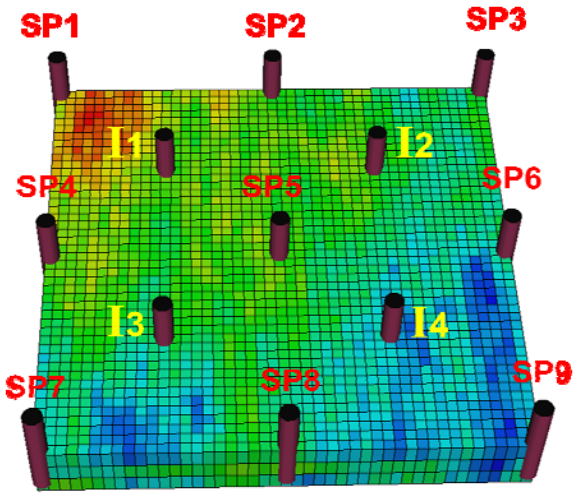

Fig. 4.1- Pseudo well configuration of the synthetic model.

Figures 4.2a-4.2c show the free gas saturation for the base case, maximized stored CO_2, and maximized sweep efficiency, respectively. It is important to note that the reported saturation profiles are obtained without assuming the presence of any pseudo wells (while the optimization is carried out using the pseudo wells).

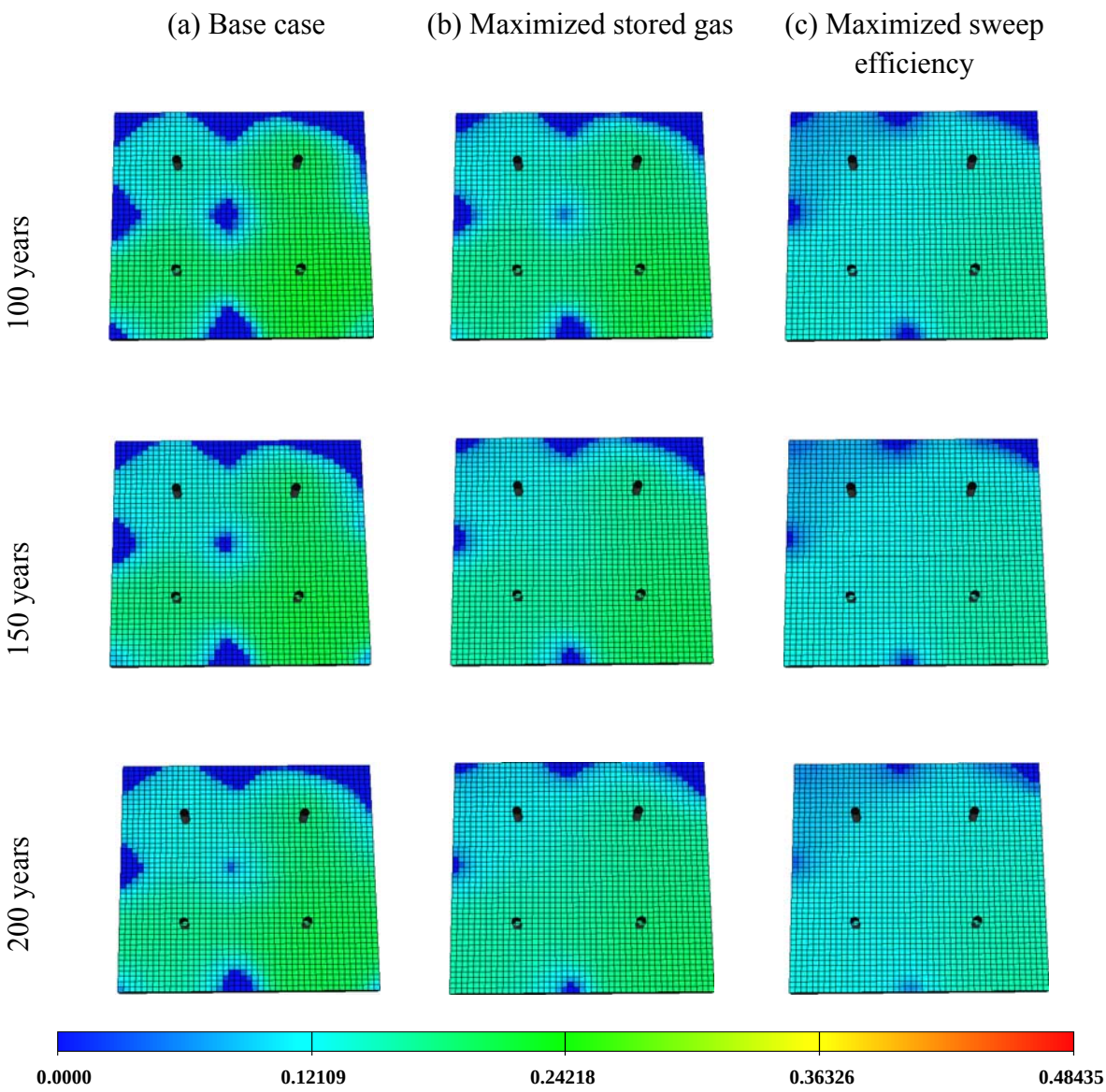

Fig.4.2- Well configuration (a) and free gas saturation for the base case (b) and maximized stored gas (c) and maximized sweep efficiency (d) for CO_2 storage after 100 years (second row), 150 years (third row), and 200 years (fourth row). The two optimized cases show less free gas relative to the base case; maximizing sweep efficiency results in an overall better spread of CO_2.

The optimized cases contain less free gas than the base case does. It is also clear from the results that the sweep efficiency optimization leads to a more uniformed distribution

of the injected CO_2, thereby enhancing the residual and solubility trapping more than maximization of the stored CO_2 can achieve.

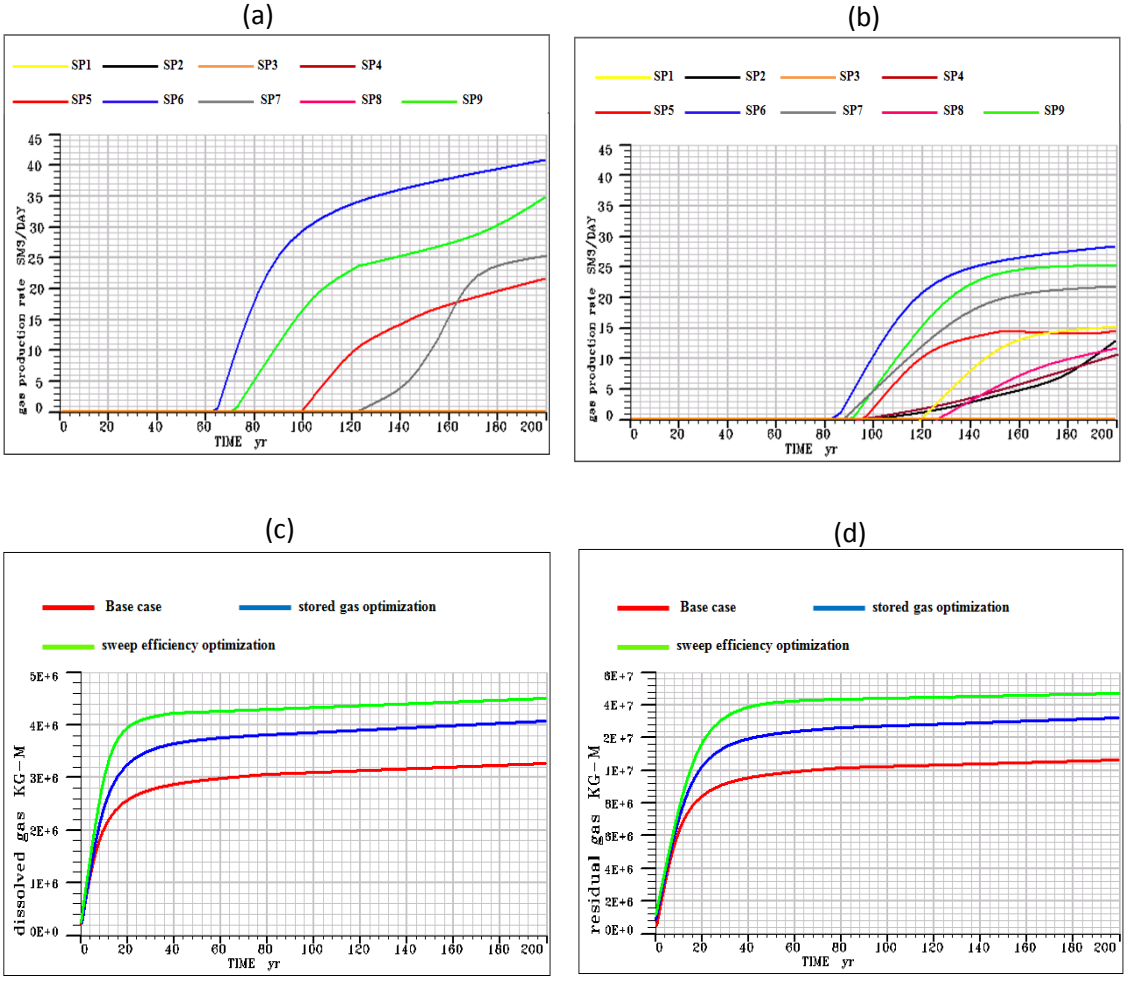

Fig .4.3- Pseudo well gas production rates before (a) and after (b) sweep efficiency optimization with the synthetic model; the resulting dissolved and residual CO2 for the base case and after maximizing the stored CO2 and sweep efficiency are shown in (c) and (d), respectively.

Figures 4.3a and 4.3b show the gas production rates at the pseudo wells before and after optimization, respectively. It is clear that the arrival time of CO_2 is delayed. However, it can also be observed that the arrival times at different wells are not equalized. This is mainly attributed to the higher mobility and lower density of the gas phase that constrains the global movement of CO_2 in the aquifer. These effects, coupled with the

limited controllability that is available in CO_2 storage problems (due to the gap between control and simulation time-scales) provide the main explanation for the variability in the CO_2 breakthrough times at different pseudo wells. Nonetheless, the optimization outcomes are markedly more desirable than those for the base case.

Figures 4.3c and 4.3d display the dissolved and residual gas for the base case, and two optimization cases (maximized stored CO_2, and maximized sweep efficiency). The improvements in the trapped residual and dissolved gas for the optimized cases relative to the base case are clearly visible in Figure 4.3.

In Figure 4.4, the optimal injection scenarios (trajectories) for the two optimization methods are shown. Clearly, the trajectory for each optimization method is different. In maximizing the sweep efficiency, Injector 1 is assigned the highest rate among all injectors at all timesteps. This injector is located in a high porosity region and is exposed to a high storage capacity. Hence, more gas is injected from Injector 1 into the top-left quadrant to achieve a more uniform sweep. Injector 4, on the other hand, has the lowest injection rate at all the timesteps. This injector is located in a low porosity area with little storage capacity; therefore, the injected gas covers the corresponding (bottom-left) quadrant of the domain rapidly. For a better sweep efficiency and similar breakthrough time, the corresponding injection rate must be sufficiently small to spread the CO_2 plume proportionally. Injectors 2 and 3 are assigned medium injection rates mainly because these two regions have mid range porosity and permeability values.

When stored CO_2 is maximized Injector 1 is again given the highest injection rate initially, because this injector is located in a region with high storage capacity. Unlike the sweep efficiency optimization, the injection rate of this injector decreases in time possibly because after a high CO_2 volume is injected in this region less storage capacity remains to store CO_2, resulting in lower injection rates at later time steps. Injector 4 has the smallest rate with and increasing trend in time. A possible justification for the

increased injection rate with time is that other injectors have higher rates and tend to utilize the storage capacity of their corresponding quadrants early during the simulation; at later times, Injector 4 has more storage capacity available relative to other injectors, which explains the increasing trend.

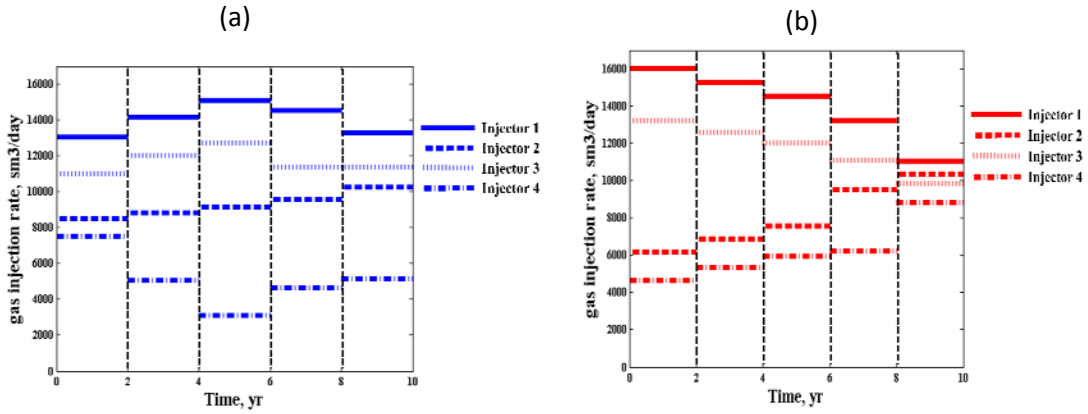

Fig. 4.4- Optimal injection scenario (trajectory) after maximizing sweep efficiency (a), and stored gas (b) for the synthetic model.

4.2 PUNQ-S3

Figure 4.5 shows the position of the injectors and the pseudo producers in the PUNQ model. The injectors are perforated in the bottom most layer and since the gas moves upward to the top most layer the pseudo wells are perforated in the top most layer.

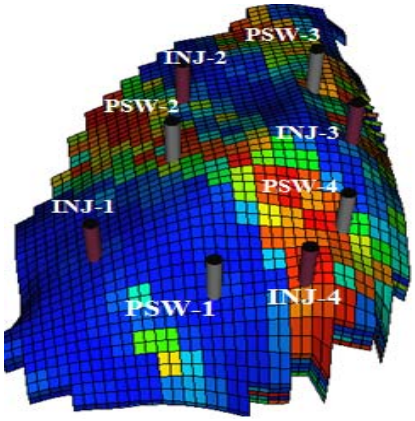

Fig. 4.5-Pseudo well configuration of the PUNQ model.

It has been shown in the literature that the size of the gridblocks is important in capturing the exact behavior of CO_2 (Juanes et al., 2006; Sifuentes et al., 2009). Therefore, it is important to use a reasonable gridsize, especially closer to CO_2 injectors where steeper changes are expected; otherwise, the simulation results may suffer from numerical errors in estimation of CO_2 saturation and be unreliable (Hassanzadeh et al., 2009). This effect is more pronounced during and shortly after the CO_2 injection period where the dominant mechanism is two-phase flow displacement, mainly because resolving the fingering effect (convection) requires high spatial resolution. Low spatial resolution may lead to overestimation of dissolution due to numerical smearing (numerical diffusion) at the CO_2 front. For our purpose, we used a 2 by 2 by 1 refinement of the original PUNQ model. The total injection time is 30 years and we inject about 50% of the pore volume of the reservoir. The total injection time is 30 years, which is divided into 5 equal timesteps. In each timestep there are 4 control variables (injection rates) and a total of 20 unknowns (controls) for the 5 optimization timesteps.

Figure 4.6 shows the free gas saturation for the base case, maximized stored CO_2 and maximized sweep efficiency, respectively, for all the layers of PUNQ model after 500 years. The optimization methods lead to less free gas at the end of simulation, implying that more gas is stored in the form of residual gas and dissolved gas. It is also evident that maximizing sweep efficiency leads to better results (less free gas).

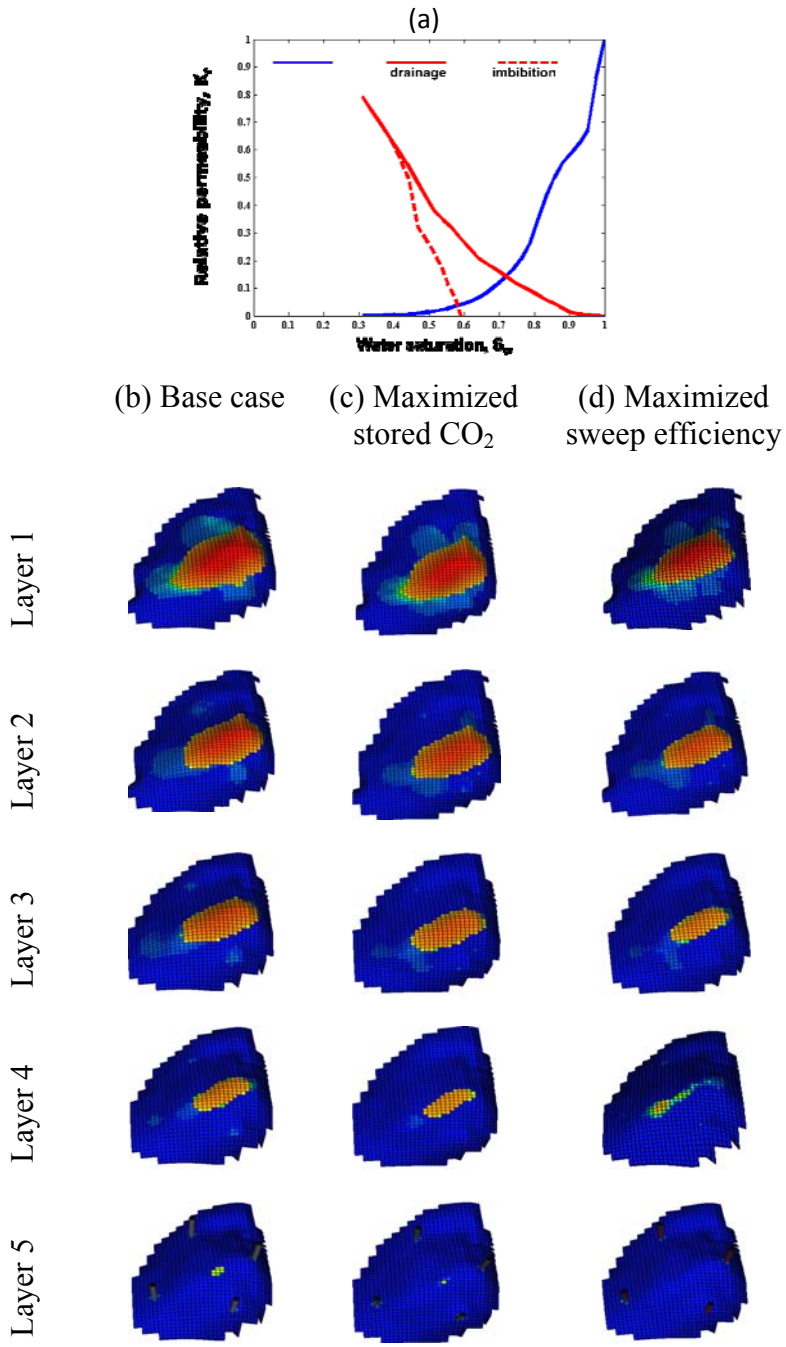

Fig. 4.6- Optimization results for CO2 sequestration with the PUNQ model: (a) saturation-dependent CO2 and brine relative permeability curves (Kilough's model is used for hysteresis); free CO2 saturation for the base case (b), maximized stored gas (c) and maximized sweep efficiency (d) are displayed. Less free gas is observed for the two optimized cases and maximization of sweep efficiency results in the least free gas.

Figures 4.7c and 4.7d show the total dissolved and residual CO_2 trapping, respectively, which can be used to confirm improved results for the maximized sweep efficiency case. Figure 4.8 shows the optimal injection scenario for the two optimization methods considered.

Figures 4.7a and 4.7b display the gas production rates at the pseudo wells before and after sweep efficiency optimization. The breakthrough of CO_2 happen at almost the same time at all wells and is delayed from about 10 years to more than 60 years.

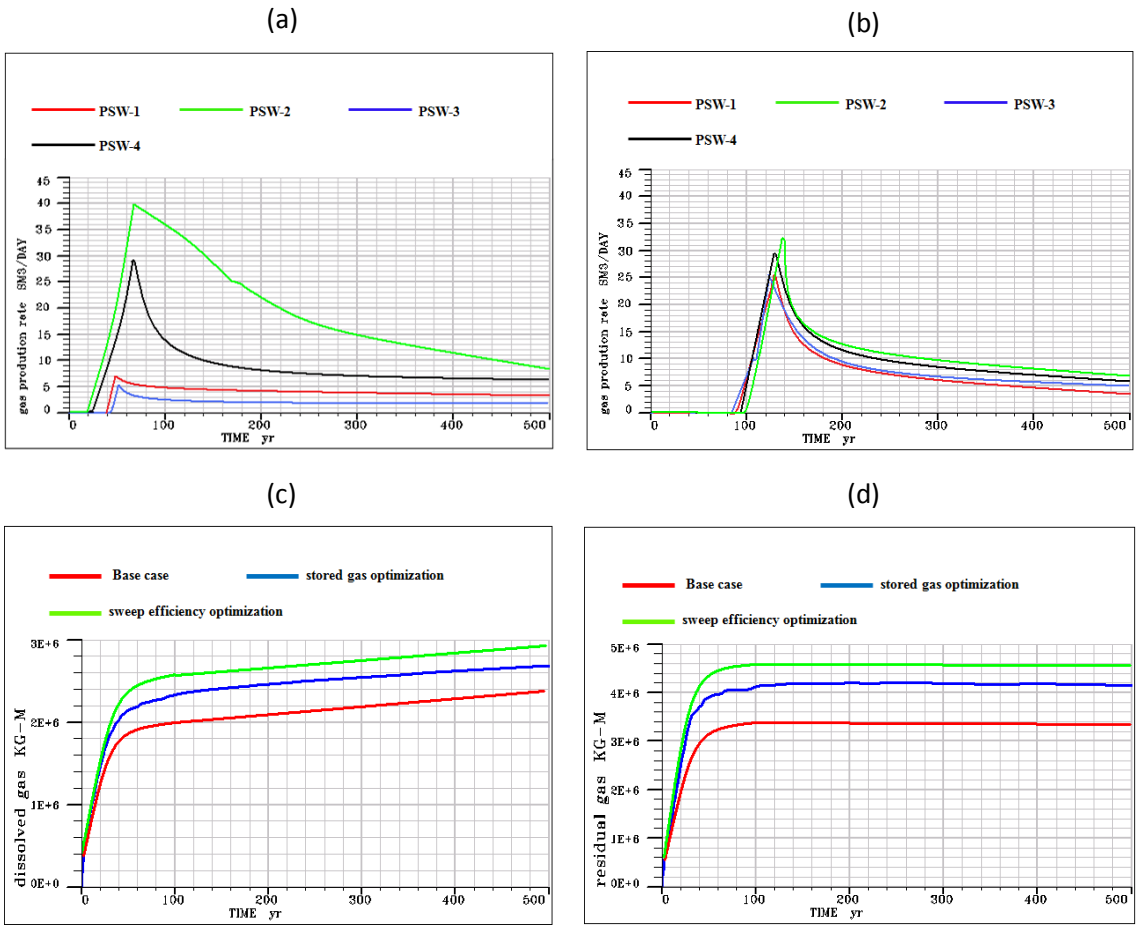

Fig. 4.7- Pseudo well gas production curves before (a) and after (b) sweep efficiency optimization with the PUNQ model; the resulting dissolved and residual CO_2 for the base case and after maximizing the stored CO_2 and sweep efficiency are shown in (c) and (d), respectively.

In the PUNQ model, the injected gas has a tendency to move upward and accumulate as free gas phase under the anticline structure on the top layer. Maximizing the sweep efficiency aims at distributing the CO_2 in a larger area of the reservoir and impeding the upward movement and accumulation of CO_2 under the cap rock. In the adopted well configuration (see Figure 4.5), Injector 4 is very close to the anticline and is located in a highly permeable path extending to the anticline. This is expected to affect the optimal solution of the sweep efficiency optimization by assigning low injection rates to this well at all timesteps (as can be verified in Figure 4.8a). On the other hand, Injector 1 is farthest from the anticline and is not connected to the anticline through a high permeability streak, which results in delayed breakthrough and, therefore, a higher injection rate assigned to it. Injector 2 is the second farthest well from the anticline and is assigned relatively high injection rates. The optimal injection rate for Injectors 1 and 2 gradually decrease in time mainly because the initial high injection rates consume the storage capacity in those regions.

In maximizing the stored CO_2 (Figure 4.8b) the algorithm targets the storage capacity of different portions of the reservoir. Since Injector 4 is located in a high porosity region the optimization algorithm chooses a relatively high rate for this injector with a decreasing trend at later timesteps. The decreasing behavior can also be explained by the proximity of this well to the anticline. Injector 2 is also located in a high porosity region and is far from the anticline; hence, a relatively high injection rate is assigned to it throughout the injection period. Finally, Injector 1 is farther from the anticline (with a combined low permeability and physical distance), had is given a steady high injection rate.

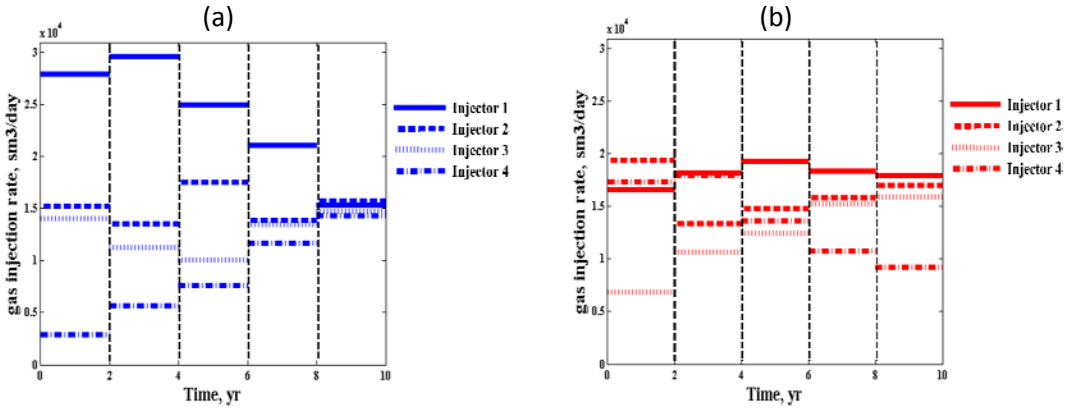

Fig. 4.8 Optimal injection scenario (trajectory) after maximizing sweep efficiency (a), and stored gas (b) for the synthetic model.

As we saw in this chapter, the new method of sweep efficiency optimization can enhance the storage of CO_2 through improving residual and solubility trapping. The two methods of CO_2 storae optimization provide different solutions because the objective functions have been defiened in different ways. In case in sweep efficiency optimization we saw that the gas production curves cannot follow that uniform behavior as they did in case of water flooding. The three below reason could be stated for this issue:

1- Higher mobility ratio in water-gas system comparing with water-oil system: Since the mobility of gas is very high the controllability of the system will be less meaning that the injection rates have less effect on managing the behavior of the gas.
2- No production control in CO_2 sequestration optimization: In waterflooding rather that the injectors we have controls on producers but in CO_2 sequestration there is no producers.
3- Difference between the timescale of controls and the objective function: We define the objective function during the whole simulation time but the impact of the controls (injection rates) are only during the injection period.

CHAPTER V

CONCLUSIONS

In this study a new optimization algorithm for maximizing the sweep efficiency of CO_2 injection into heterogeneous saline aquifers or reservoirs. The proposed method is applicable to optimization of sweep efficiency in both waterflooding and CO_2 sequestration projects. The general idea is to find optimal injection/production scenarios that lead to delayed and equalized breakthrough times in all production or monitoring wells. In the case of CO_2 sequestration, pseudo production wells with very small (negligible) production rates (to avoid disturbing the overall flow regime) are placed in the aquifer to quantify the breakthrough of injected fluid at selected locations. The objective function in waterflooding optimization is the misfit between water production rates (to equalize breakthrough times) augmented by a term to minimize the total field water production (thereby delaying water breakthrough). This objective function is minimized by controlling the injection and production rates or well bottomhole pressures depending on problem setup. The application of this method to waterflooding experiments in a 3D synthetic model and a more realistic formation (PUNQ model) has shown that the new method can successfully achieve a uniform sweep efficiency, resulting in equalized and delayed breakthrough times. The synthetic model allowed for introduction of a well grouping concept to better implement the algorithm while the PUNQ model offered an opportunity to evaluate the performance of the optimization algorithm in a highly heterogeneous formation where well placement and grouping is not obvious.

The introduction of pseudo wells in CO_2 sequestration allows us to apply the proposed algorithm to geologic CO_2 storage problems. The CO_2 sequestration problem has distinct properties that distinguish it from waterflooding problems. Among these important differences, the sharp density contrast between the brine and injected CO_2 leads to a

dominant upward migration of the CO_2 plume from the injection point to the top layer of the aquifer. The dominant upward flow regime constrains the ability of the optimization problem in achieving good sweep efficiency and mobilizing CO_2 plume in the lateral direction. In addition, since the time-scale of CO_2 injection period (which is also the control time) is orders of magnitude less than the time it takes to achieve permanent storage (which needs to be simulated in calculating the desired objective function), there is a small scope (and time interval) for controlling the storage performance of the aquifer far into the future. Despite these challenging aspects of optimizing sweep efficiency and performance of CO_2 storage we obtained significant improvement in improving solubility and residula trapping by improving the sweep efficiency.

Overall, successful application of the proposed optimization method to two heterogeneous models in this paper suggests that that an optimal rate allocation can mitigate the challenges in increasing the storage capacity of saline aquifers when a reliable model exists to capture the heterogeneity in aquifer properties. Generation of such predictive models would require integration of various sources of data from static well measurements to dynamic monitoring data, tracer test data, and time-lapse seismic surveys. Once a reasonable predictive model is constructed, the optimization approach proposed in this paper can be used to guide the injection rate allocation problem in large scale field applications where several injection wells may be used to store CO_2 in complex geologic formations. The complexity associated with heterogeneity and spatial variability of aquifer transport properties at several scales, together with the inaccessibility and high cost of direct sampling, leads to significant uncertainty and systematic errors in subsurface characterization studies, hence modeling CO_2 displacement behavior. An important addition to the proposed problem formulation currently under investigation is accounting for the uncertainty in the description of subsurface heterogeneity, which can be quite significant in realistic problems.

REFERENCES

Alhuthali, A.H., Oyerinde, D. and Datta-Gupta, A. 2007. Optimal Waterflood Management Using Rate Control. Paper SPE 102478 presented at SPE Reservoir Evaluation & Engineering. New Orleans, 15-18 October.

Allis, R.G., Chidsey, T., Gwynn, W., Morgan, C., White, S.P., Adams, M., and Moore, J. 2001. Natural CO_2 Reservoirs on the Colorado Plateau and Southern Rocky Mountains. Paper presented at the 1st National Conference on Carbon Sequestration, Washington, DC, May 14-17.

Anchliya, A., Ehlig-Economides, C. and Jafarpour, B. 2010. Aquifer Management to Accelerate CO_2 Dissolution and Trapping. Submitted to *SPE Journal*.

Arenas A. and Dolle N. 2003. Smart Waterflooding Tight Fractured Reservoirs Using Inflow Control Valves. Paper SPE 84193 presented at the SPE Annual Technical Conference and Exhibition held in Denver, CO, 20-23 October.

Bachu, S. and Adams, J. J. 2003. Sequestration of CO_2 in Geological Media in Response to Climate Change: Capacity of Deep Saline Aquifers to Sequester CO_2 in Solution. *Energy Conversion and Management* **44**(20): 3151–3175.

Bachu, S., 2000. Sequestration of CO_2 in Geological Media: Criteria and Approach for Site Selection in Response to Climate Change, *Energy Conversion and Management*, **41**: 953-970.

Bachu, S. 2002. Sequestration of CO_2 in Geological Media in Response to Climate Change: Road Map for Site Selection Using the Transform of the Geological Space into CO_2 Phase Space. *Energy Convers. Mgmt*. **43**: 87-102.

Bachu, S., and Adams, J.J., 2003. Sequestration of CO_2 in Geological Media in Response to Climate Change: Capacity of Deep Saline Aquifers to Sequester CO_2 in Solution. *Energy Convers. Mgmt.* **44**: 3151-3175.

Bachu, S., Gunter, W.D. and Perkins, E.H. 1994. Aquifer Disposal of CO_2 Hydrodynamic and Mineral Trapping. *Energy Conversion and Management* **35**: 269-279.

Bergman, P. D., and Winter, E. M. 1995. Disposal of CO_2 in Aquifers in the U.S. *Energy Convers. Mgm.* **36**: 523-526.

Bergman, P. D., Winter, E. M., and Chen, Z. Y. 1997. Disposal of Power Plant CO_2 in Depleted Oil and Gas Reservoirs in Texas. *Energy Convers. Mgmt.* **38**: 211-216.

Brouwer D. R. and Jansen J. D., 2002. Dynamic Optimization of Waterflooding with Smart Wells Using Optimal Control Theory, Paper SPE 78278 presented at the 2002 SPE European Petroleum Conference, Aberdeen, 17-20 December.

Brouwer, D. R., Jansen J. D., Van Der Starre, S., van Kruijsdijk, S. and Berentsen, C. W. J. 2001. Recovery Increase through Waterflooding with Smart Well Technology. Paper SPE 68979 presented at the SPE European Formation Damage Conference, The Hague, The Netherlands, 8-11 September.

Brouwer, D. R., Jansen, J. D., Van Der Starre, S., van Kruijsdijk, and Berentsen, C. W. J., 2001. Recovery Increase through Waterflooding with Smart Well Technology. Paper SPE 68979 presented at the SPE European Formation Damage Conference, The Hague, The Netherlands, 10-12 November.

Brouwer, D.R., Naevdal, G., Jansen, J.D., Vefring, E.H. and van Kruijsdijk, C.P.J.W. 2004. Improved Reservoir Management Through Optimal Control and Continuous Model Updating. Paper SPE90149 presented at the SPE Annual Technical Conference and Exhibition, Houston, TX, 26-29 September.

Bryant, S.L., Lakshiminarasimhan, S., and Pope, G.A. 2006. Buoyancy-Dominated Multiphase Flow and Its Impact on Geological Sequestration of CO_2. .Paper SPE 99938 presented at the SPE/DOE Symposium on Improved Oil Recovery, Tulsa, 22–26 April.

Doughty, C., Pruess, K., Benson, S. M., Hovorka, S. D., Knox, P. R. and Green, C. T. 2001. Capacity Investigation of Brine-bearing Sands of the Frio Formation for Geologic Sequestration of CO_2. Proceedings of First National Conference on Carbon Sequestration DOE-NETL, CD-ROM USDOE/ NETL-2001/1144, Washington, D.C. 14–17 May.

Drange, H., Alendal, G. and Johannessen, O.M., 2001. Ocean Release of Fossil Fuel CO_2: A Case Study. *Geophysical Research Letters* **28**: 2637-2640.

Duan, Z. and Sun, R., 2003. An Improved Model Calculating CO_2 Solubility in Pure Water and Aqueous NaCl Solutions from 273 to 533 K and from 0 to 2000 bar. *Chemical Geology*, **193**: 257-271.

Enick, R.M. and S.M. Klara, 1990. CO_2 Solubility in Water and Brine under Reservoir Conditions. *Chemical Engineering Communications*, **90**: 23–33.

Ennis-King, J.P. and L. Paterson, 2003. Role of Convective Mixing in the Long-term Storage of Carbon Dioxide in Deep Saline Formations. Presented at Society of Petroleum Engineers Annual Technical Conference and Exhibition, SPE 84344, Denver, Colorado.

Esmaiel, T. E. H.,2005. Applications of Experimental Design in Reservoir Management of Smart Wells. Paper SPE 94838 presented at the SPE Latin American and Caribbean Petroleum Engineering Conference, Rio de Janeiro, Brazil, 12-14 May.

Fathi, Z., and Ramirez, W. F. 1984. Optimal Injection Policies for Enhanced Oil Recovery: Part 2 – Surfactant Flooding. *SPE Journal*, 333-341.

Francey, R.J., Allison, C.E., Etheridge, D.M., Trudinger, C.M., Enting, I.G., Leuenberger, M., Langenfelds, R.L., Michel, E. and Steele, L.P. 1999. A 1000-year High Precision Record of δ13C in Atmospheric CO2. *Tellus* **51**B: 170–193.

Gale, J. and Freund, P., 2001. Coal-bed Methane Enhancement with CO2 Sequestration Worldwide Potential. *Environmental Geosciences* **8**: 210-217.

Glandt, C. A., 2003. Reservoir Aspects of Smart Wells. Paper SPE 81107 presented at the SPE Latin American and Caribbean Petroleum Engineering Conference, Port-of-Spain, Trinidad, West Indies, 23-26 November.

Gunter, W. D., Perkins, E. H., and Hutcheon, I. 2000. Aquifer Disposal of Acid Gases: Modeling of Water-Rock Reactions for Trapping of Acid Wastes. *Applied Geochemistry* **15**: 1085-1095.

Gunter, W. D., Wiwchar, B., and Perkins, E. H. 1997. Aquifer Disposal of CO_2-rich Greenhouse Gases: Extension of the Time Scale of Experiment for CO_2- sequestering Reactions by Geochemical Modeling. *Mineralogy and Petrology* **59**: 121-140.

Gunter, W.D., Bachu, S., Law, D.H.-S., Marwaha, V., Drysdale, D.L., Macdonald, D.L. and McCann, T.J. 1996. Technical and Economic Feasibility of CO_2 Disposal in

Aquifers within the Alberta Sedimentary Basin, Canada. *Energy Conversion and Management* **37**: 1135-1142.

Gunter, W.D., Perkins, E.H. and McCann, T.J. 1993. Aquifer Disposal of CO_2-Rich Gases: Reaction Design for Added Capacity. *Energy Conversion and Management* **34**: 941- 948.

Harding, T. J., Radcliffe, N. J., and King, P. R., 1998. Hydrocarbon Production Scheduling with Genetic Algorithms. *SPE Journal* **3**(2): 99 – 107.

Hassanzadeh, H., Pooladi-Darvish, M., and Keith, D.W., 2009. Accelerating CO_2 Dissolution in Saline Aquifers for Geological Storage-Mechanistic and Sensitivity Studies. *Energy & Fuels* **23**: 3328–3336.

Holloway, S. and Savage, D. 1993. The Potential for Aquifer Disposal of Carbon Dioxide in the UK. *Energy Conversion and Management* **34**: 925-932.

Holt, T., J.L. Jensen and E. Lindeberg, 1995. Underground Storage of CO_2 in Aquifers and Oil Reservoirs. *Energy Conversion and Management* **36**(6–9): 535–538.

Holtz, M.H. 2002. Residual Gas Saturation to Aquifer Influx: A Calculation Method for 3-D Computer Reservoir Model Construction. Paper SPE 75502, presented at the SPE Gas Technologies Symposium, Calgary, Alberta, Canada. 12-14 September.

IPCC, 2005. IPCC Special Report on Carbon Dioxide Capture and Storage, Summary for Policy Makers, Intergovernmental Panel on Climate Change. 235-305.

Juanes, R., Spiteri, E. J., Orr, F. M., and Blunt, M. J., 2006. Impact of Relative Permeability Hysteresis on Geological CO2 Storage. *Water Resources Research* **42**(12): 436-448.

Keeling, C. D. 1960. The Concentration and Isotopic Abundances of Carbon Dioxide in the Atmosphere. *Tellus* **12**: 200-203.

Keeling, C. D. 1976. Atmospheric Carbon Dioxide Variations at Mauna Loa Observatory. *Tellus* **28**: 538-51.

Keith, D., Hassanzadeh, H. and Pooladi-Darvish, M. 2005. Reservoir Engineering to Accelerate Dissolution of Stored CO_2 in Brines. Proceedings of the 7th International Conference on Greenhouse Gas Control Technologies (GHGT-7), September 5–9, 2004, Vancouver, Canada, **2**: 2163-2168.

Killough, J. E. 1976. Reservoir Simulation with History-dependent Saturation Functions. *Soc. Pet. Eng. J.* **16**(1): 37–48.

Klusman, R.W. 2003. Evaluation of Leakage Potential from a Carbon Dioxide EOR/Sequestration Project. *Energy Conversion and Management* **44**: 1921-1940.

Koide, H.G., Takahashi, M. and Tsukamoto, H. 1995. Self-trapping Mechanisms of Carbon Dioxide. *Energy Conversion and Management* **36**(6–9), 505–508.

Kumar, A., Ozah, R., Noh, M., Pope, G.A., Bryant, S., Sepehrnoori, K. and Lake, L., 2005. Reservoir Simulation of CO_2 Storage in Deep Saline Aquifers. *SPEJ,* **10**: 336-348.

Lackner, K.S., 2002. Carbonate Chemistry for Sequestering Fossil Carbon. *Annual Review of Energy and the Environment* **27**: 193-232.

Lee, A. S. and Aronofsky, J. S., 1958. A Linear Programming Model for Scheduling Crude Oil Production. *Journal of Petroleum Technology* **10**(7): 51-54.

Leonenkoy, Y. and Keith, D. 2008. Reservoir Engineering to Accelerate the Dissolution of CO_2 Stored in Aquifers. *Environ. Sci. Technol*. **42**: 2742-2747.

Lindeberg, E. and Wessel-Berg, D. 1997. Vertical Convection in an Aquifer Column under a Gas Cap of CO_2. *Energy Conversion and Management* **38**(Suppl.): S229–S234.

McMillan B., and Bryant, S. 2007. Surface Mixing as Method for Minimizing Risk in CO_2 Sequestration. Proceedings of the Six Annual Conference on Carbon Capture and Sequestration, Pittsburg, PA, 7-10 May.

McPherson, B. J. O. L., and Cole, B. S. 2000. Multiphase CO_2 Flow, Transport and Sequestration in the Powder River Basin, Wyoming, U.S.A. *Journal of Geochemical Exploration* **69**: 65-69.

Metz, B., Davidson, O., de Coninck, H., Loos, M. and Meyer, L.A. 2008. Special Report on Carbon Dioxide Capture and Storage, Intergovernmental Panel on Climate Change, Cambridge, UK and New York.

Nghiem, L., Sammon, P., Grabenstetter, J., and Ohkuma, H. 2004. Modeling CO_2 Storage in Aquifers with a Fully-Coupled Geochemical EOS Compositional Simulator, Paper SPE 89474 presented at the SPE/DOE Symposium on Improved Oil Recovery, Tulsa, Oklahoma, 17-21 April.

Nocedal, J., and Wright, S.J. 2006. *Numerical Optimization,* 2nd ed., Series in Operations Research and Financial Engineering. Springer, New York.

Obdam, A., van der Meer, L. G. H., May, F., Kervevan, C., Bech, N. and Wildenborg, A. 2002. Effective CO_2 Storage Capacity in Aquifers, Gas Fields, Oil Fields and Coal Fields. Proceedings of the 6th International Conference on Greenhouse Gas Control Technologies (GHGT-6), J. Gale and Y. Kaya (eds.), 1–4 October, Kyoto, Japan, Pergamon, **1**: 339–344.

Obi, E-O.J. and Blunt, M.J., 2006. Streamline-Based Simulation of Carbon Dioxide Storage in a North Sea Aquifer. *Water Resources Research* **42**: W03414.

Pawar, R., Warpinski, N., Benson, R., Grigg, R., New Stubbs, B., Krumhansl, J. Lorenz, J., Svec, R., Stauffer, P., Zhang, D., and Westrich, H. 2004. Geologic Sequestration of CO_2 in West Pearl Queen Field: Results of a Field Demonstration Project. Paper presented at the Third Annual Conference on Carbon Dioxide Sequestration, Alexandria, VA, 3-6 May.

Pearce, J.M., Holloway, S., Wacker, H., Nelis, M.K., Rochelle, C., and Bateman, K. 1996. Natural Occurrences as Analogues for the Geological Disposal of Carbon Dioxide. *Energy Convers.Mgmt.* **37**(6-8), 1123 - 1128.

PUNQ-S3website: (Accessed 22 October 2010)
(http://www3.imperial.ac.uk/earthscienceandengineering/research/perm/punq-s3model

Qi, R., Beraldo, V., LaForce, T. and Blunt, M.J. 2007. Design of Carbon Dioxide Storage in a North Sea Aquifer Using Streamline-Based Simulation, Paper SPE 109905 presented at the Proceedings of the Annual Technical Conference and Exhibition, Anaheim, CA, 11–14 November.

Ramirez, W. F., Fathi, Z., and Cagnol, J. L, 1984. Optimal Injection Policies for Enhanced Oil Recovery: Part 1 – Theory and Computational Strategies. *SPE Journal*, 328-332.

Saripalli, P, and McGrail, B.P. 2002. Semi-Analytical Approaches to Modeling Deep Well Injection of CO_2 for Geological Sequestration. *Energy Conversion and Management* **43**(2): 185-198.

Sarma, P., Aziz K., and Durlofsky, L. J. 2005. Implementation of Adjoint Solution for Optimal Control of Smart Wells. Paper SPE 92864 presented at the 2005 SPE Reservoir Simulation Symposium, Houston, TX, 10-12 May.

Sarma, P., Durlofsky, L.J., Aziz, K. and Chen, W.C. 2006. Efficient Real-time Reservoir Management Using Adjoint-based Optimal Control and Model Updating. *Computational Geosciences* **10**: 3-36.

Seneviratne, G. 2003. Global Warming and Terrestrial Carbon Sequestration. *Journal of Biosciences* **28**: 653-655.

Sifuentes, W., Blunt, M.J. and Giddins, M.A. 2009. Modeling CO_2 Storage in Aquifers: Assessing the Key Contributors to Uncertainty. SPE paper 123582 presented at the Offshore Europe Conference, Aberdeen, UK, 8-11 September.

Stuiver, M., Burk, R. L. and Quay, P. D. 1984. 13C/12C Ratios and the Transfer of Biospheric Carbon to the Atmosphere. *J. Geophys. Res.* **89**: 1731–1748.

Tavakkolian, M., Jalali, F., and Amadi, M. A. 2004. Production Optimization Using Genetic Algorithm Approach. Paper SPE 88901 presented at the 28th Annual SPE International Technical Conference Exhibition, Abuja, Nigeria, 2-4 August.

Thibeau, S., Nghiem, L.X. and Ohkuma, H. 2007. A Modeling Study of Selected Minerals in Enhancing CO_2 Mineralization During CO_2 Aquifer Storage. Paper SPE 109739 presented at the SPE Annual Technical Conference and Exhibition, Anaheim, CA, 11-14 November.

Vesovic, V., Wakeham, W. A., Olchowy, G.A., Sengers, J.V., Watson, J.T.R. and Millat, J. 1990. The Transport Properties of Carbon Dioxide. *J. Phys. Chem. Ref. Data* **19**(3): 234-248.

Wattenbarger, R. A., 1969. Maximizing Seasonal Withdrawals from Gas Storage Reservoirs. Paper SPE 2406 presented at SPE 44th Annual Fall Meeting, Denver, CO, 21-23 September.

Weir, G. J., White, S. P., and Kissling, W. M. 1996. Reservoir Storage and Containment of Greenhouse Gases. *Transport in Porous Media* **23**: 37−60.

Weir, G.J., White, S.P. and Kissling, W.M. 1995. Reservoir Storage and Containment of Greenhouse Gases. *Energy Conversion and Management* **36**: 531-534.

Zaytsev, I.D. and Aseyev, G.G. 2005. Properties of Aqueous Solutions of Electrolytes. *Geochimica et Cosmochimica Acta* **69**(13): 3309-3320.

Zhou, C., Gao, C., Jin, Z., and Wu, X. 1992. A Simulated Annealing Approach to Constrained Nonlinear Optimization of Formation Parameters in Quantitative Log

Evaluation. Paper SPE 24723 presented at the 67th Annual Technical Conference and Exhibition, Washington, DC, 4-9 October.

VITA

Name:	Hossein Shamshiri
Address:	Richardson Building Department of Petroleum Engineering Texas A&M University College Station, TX 77843-3116
Email Address:	hossein.shamshiri@pe.tamu.edu
Education:	B.S., Petroleum Engineering, Petroleum University of Technology, 2008 M.S., Petroleum Engineering, Texas A&M University, 2010